

We are IntechOpen, the world's leading publisher of Open Access books Built by scientists, for scientists

6,900

Open access books available

185,000

International authors and editors

200M

Downloads

Our authors are among the

154

Countries delivered to

TOP 1%

most cited scientists

12.2%

Contributors from top 500 universities



WEB OF SCIENCE™

Selection of our books indexed in the Book Citation Index
in Web of Science™ Core Collection (BKCI)

Interested in publishing with us?
Contact book.department@intechopen.com

Numbers displayed above are based on latest data collected.
For more information visit www.intechopen.com



A Novel Multiclad Single Mode Optical Fibers for Broadband Optical Networks

Rostami^{1,2} and S. Makouei¹

¹*Photonics and Nanocrystal Research Lab. (PNRL), Faculty of Electrical and Computer Engineering, University of Tabriz, Tabriz 51666,*

²*School of Engineering-Emerging Technologies, University of Tabriz, Tabriz 51666, Iran*

1. Introduction

The demand for data communication is growing rapidly due to the increasing popularity of the Internet and other factors [1]. The unprecedented success of information technology in recent years ushers an explosive growth in demand for the Internet access in the 21st century. Ultra-wideband transmission media are needed in order to provide high-speed communications for a much larger number of users. A promising solution to the capacity crunch can come from wavelength-division-multiplexed optical fiber communication systems that are shown to provide enormous capacities on the order of terabit per second over long distances. These systems utilize single-mode fibers, in conjunction with erbium-doped fiber amplifiers, as the transmission medium [2]. The optical silica fiber might be the only proper choice to realize this task. Optical fiber based communication is the excellent alternative for these purposes which needs low dispersion as well as dispersion slope and large bandwidth supported by optical physical medium[3]. Optical transmission began to be used in trunk cables about 1990; the capacity of those systems was several hundred Mbit/s per fiber. The capacity jumped to 2.5 (5.0) Gbit/s per fiber with the introduction of optical repeaters using erbium-doped fiber amplifiers in 1995. It jumped again in 1998, to 10 (20) Gbit/s per fiber, with the introduction of wavelength division multiplexing (WDM) [5]. Overall transmission capacity now exceeds 100 Gbit/s per fiber due to improvements in WDM techniques [6]. Usually, those techniques are called dense WDM (DWDM). In recent years, the increasing demands for transmission capacity have led to intense research activities on high capacity DWDM communication system [7].

Nowadays, applications such as optical time division multiplexing (OTDM) and dense wavelength division multiplexing (DWDM) are usual tasks in industry [1]. Therefore by considering these applications, providing a large bandwidth and high-speed communication possibility using optical fibers is highly interesting [3].

In the following, we review requirements for DWDM, Dispersion properties, optical nonlinearity, loss properties, and design of optical fiber for DWDM.

2. Requirements for DWDM

The number of wavelengths (channels) in the fibers of DWDM systems is increasing. As discussed earlier, a WDM signal typically occupies a bandwidth of 30 nm or more, although

Source: Advances in Solid State Circuits Technologies, Book edited by: Paul K. Chu,
ISBN 978-953-307-086-5, pp. 446, April 2010, INTECH, Croatia, downloaded from SCIYO.COM

it is bunched in spectral packets of bandwidth ~ 0.1 nm (depending on the bit rate of individual channels) [1]. To use such new optical transmission systems, the DWDM fiber should overcome three transmission related limitations: dispersion, optical fiber nonlinearity and loss properties. For 10-Gb/s channels, the third-order dispersion does not play an important role as relatively wide (> 10 ps) optical pulses are used for individual channels. However, because of the wavelength dependence of β_2 , or the dispersion parameter D , the accumulated dispersion will be different for each channel [4]. Wavelength division multiplexing (WDM) systems have been widely introduced for large capacity transmission. In order to further increase the transmission capacity, several techniques have been investigated, such as higher bit-rate transmission [8], enhancement of the spectral efficiency [9], and use of new transmission bands [10, 11]. In those systems, optical fibers are required more strongly to reduce the nonlinearity and the dispersion slope [5].

3. Dispersion properties

Silica fibers suffer from some disadvantages especially dispersion and dispersion slope. Meanwhile, these two factors cause severe restrictions for high-speed pulse propagation [1]. The dispersion value becomes larger by the wavelength increasing in the conventional optical fibers. So owing to the dissimilar broadening for different channels, the multi-channel application realization would be hard. A suitable optical fiber should meet the small dispersion as well as the small dispersion slope in the predefined wavelength interval. The dispersion properties are the dispersion itself and the dispersion slope of the optical fiber. The dispersion value cannot be in the zero-value region because FWM causes interaction between signals (optical channels) in DWDM systems when there is phase matching between the optical channels due to zero dispersion. Therefore, the dispersion value in the signal wavelength region must have the proper non-zero value. The sign of the dispersion value should be positive for short-distance transmission and negative for ultra-long-distance transmission [12] because of modulation instability in the positive dispersion in a long link. When the signal wavelength band becomes wider, the difference in the dispersion values at the edges of the wavelength band becomes larger. Dispersion compensation thus becomes difficult for long distance DWDM transmission. To achieve both long distance and high speed transmission with easy dispersion compensation for a wide wavelength band, the dispersion slope should be reduced. For single wavelength communication, dispersion shifted fiber is enough. But for applications such as DWDM this method cannot provide high speed possibility. In these applications, the physical media should provide the flat, minimum, and uniform dispersion as well as dispersion slope ideally. An important limitation induced by chromatic dispersion and its slope is broadening factor which restricts the bit rate parameter.

To minimize pulse broadening in an optical fiber, the chromatic dispersion should be low over the wavelength range used. A fiber in which the chromatic dispersion is low over a broad wavelength range is called a dispersion-flattened fiber.

4. Optical nonlinearity

The response of any dielectric to light becomes nonlinear for intense electromagnetic fields, and optical fibers are no exception. Even though silica is intrinsically not a highly nonlinear material, the waveguide geometry that confines light to a small cross section over long fiber

lengths makes nonlinear effects quite important in the design of modern light wave systems [1]. The much higher power level due to simultaneous transmission of multiplexed channels and propagation over much longer distances made possible with the utilization of fiber amplifiers, cause the otherwise weak and negligible fiber nonlinearities to affect the signal transmission significantly [2]. When the number of signal wavelengths carried in an optical fiber increases, the average transmission power density becomes larger than that in conventional systems. Consequently, optical-fiber nonlinearities have emerged as a main issue. This nonlinearity seriously limits transmission capacity with various nonlinear interactions, which are generally categorized as scattering effects and optical signal interactive modulation. Because the signal power density is stronger due to the greater number of channels in DWDM systems, optical fiber nonlinearity limits the number/spacing of the channels and the length/speed of the transmission. In general, the refractive index of optical fiber has a weak dependence on optical intensity (equal to signal power (p) per effective area (A_{eff}) in the fiber. Optical fiber nonlinearity arises from modulation of the refractive index caused by changes in the optical intensity of the signal. This cause four wave mixing (FWM), self-phase modulation (SPM) and cross phase modulation (XPM) can be observed in the fiber. The XPM and SPM distort the signals. Therefore, optical fiber nonlinearity must be reduced. The most practical way to do this is to enlarge A_{eff} [13]. The relationship between A_{eff} and mode field diameter (MFD) is direct and proportional. As a result, enlarging MFD is a practical solution for low nonlinearity. The choice of dispersion shifted fibers (DSFs) along with erbium-doped fiber amplifiers (EDFAs), for operation at 1550nm window, would be an ideal one to achieve greater transmission distance and utilize full capacity of transmission system [5,7,15]. However, when the system is operated at the zero dispersion wavelengths, the nonlinear interaction between the channels and noise components is increased. The system working slightly away from the zero dispersion wavelengths can reduce these unwanted interactions. The WDM system reduces the nonlinear effects and enables multi-wavelength transmission through non-zero dispersion shifted fibers having very small dispersion in duration 1530-1610 nm. In order to increase the information carrying capacity, latest high speed communication system is based on the dense wavelength division multiplexing/demultiplexing (DWDM) [16, 17]. In such systems, nonlinear effects like four wave mixing (FWM), which arise due to simultaneous transmission at many closely spaced wavelengths and high optical gain from EDFA, imposes serious limitations on the use of a DSF with zero dispersion wavelength at 1550 nm [18,19]. To overcome this difficulty, the nonzero dispersion shifted fibers having small dispersion in the range $\sim 2\text{--}4$ ps/km/nm over the entire gain window of EDFA have been proposed [20, 21]. In such fibers, the phase matching condition is not satisfied and hence the effect of FWM becomes negligible due to small dispersion [15].

5. Loss properties

Progress in optical fiber fabrication technologies has resulted in a routine production of low loss single mode fibers. This enables us to apply the single mode fibers promisingly in high bit rate and long haul optical transmission systems. Structural optimization must be established so as to provide desirable transmission characteristics for given operating conditions. A basic design consideration has been made by taking into account transmission characteristics such as fiber intrinsic loss, bending loss, splice loss, and launching efficiency [22, 23]. Use of commercially available erbium doped fiber amplifiers (EDFA), which forces

optical communication systems to be operated in the 1550 nm window, has significantly reduced the link length limitation imposed by attenuation in the optical fiber [15]. The fiber loss is one of the significant restrictions in the optical fiber communication links. It is one of some reasons limit the maximum distance that information can be sent without presence of the repeaters. Meanwhile, due to the loss, the pulse amplitude reduces so that the initial information cannot be restored in the noisy conditions. Seeing that, in the fiber design one likes to shift the zero dispersion wavelength to the region that the fiber has the lowest level attenuation. The combination of natural attenuations has a global minimum around 1.55 μm and that is why most optical communication systems are operated at this wavelength [4, 18]. A kind of loss which must be taken into account in fiber design is the bending loss. Every time an optical fiber is bent, radiation occurs. When a bent occurs, a portion of the power propagating in the cladding is lost through radiation.

6. Design of DWDM fiber

There are three methods to increase the capacity of a DWDM transmission system, using a broad wavelength range, narrowing channel spacing and increasing a bit rate per channel. However, one of disadvantages for the last two methods is the degradation of the transmission performance due to optical nonlinear effects. In this area, there are three categories which cover all designs. There are based on using zero dispersion shifted fibers (ZDSFs), non-zero dispersion shifted fiber (NZDSFs) and dispersion flattened fibers (DFFs).

7. Zero Dispersion Shifted Fibers (ZDSFs)

Use of commercially available erbium doped fiber amplifiers (EDFA), which forces optical communication systems to be operated in the 1550 nm window, has significantly reduced the link length limitation imposed by attenuation in the optical fiber. However, high bit rate (~ 10 Gb/s) data transmission can be limited by the large inherent dispersion of the fiber. Dispersion shifted fibers (DSF), which has zero dispersion around 1550 nm, have been proposed and developed to overcome this problem. Dispersion shifted fiber for single wavelength optical communication is a proper choice. The much higher power level due to simultaneous transmission of multiplexed channels and propagation over much longer distances made possible with the utilization of fiber amplifiers, cause the otherwise weak and negligible fiber nonlinearities to affect the signal transmission significantly. The effects of fiber nonlinearities on pulse propagation and on the capacity of fiber optic communication systems have been studied extensively by many researchers. To mitigate the nonlinear effects in long fiber optic communication systems by zero dispersion shifted fiber, a new generation of optical fibers, referred to as large effective area fibers, has been introduced. As said earlier, in order to reduce nonlinear effects, it is preferred to increase effective area. Gathering zero dispersion and large effective area together will be an appropriate solution in this task. The large effective area fibers allow a much smaller light intensity inside the guiding region, thus resulting in less refractive index nonlinearity than the conventional single mode fibers. In addition to reduced nonlinearities, large effective area fibers must also provide low attenuation, low bending and micro-bending losses, low chromatic dispersion, and low polarization mode dispersion. In recent years, a variety of large effective area fiber designs have been reported in the literature. These designs may be broadly classified into two groups based on their refractive index profiles; R-type and M-

type. Each of two types is divided to two other categories too named type I and II. A small pulse broadening factor (small dispersion and dispersion slope), as well as small nonlinearity (large effective area) and low bending loss (small mode field diameter) are required as the design parameters in Zero dispersion shifted fibers [24]. The performance of a design may be assessed in terms of the quality factor. This dimensionless factor determines the trade-off between mode field diameter, which is an indicator of bending loss and effective area, which provides a measure of signal distortion owing to nonlinearity [25]. It is also difficult to realize a dispersion shifted fiber while achieving small dispersion slope. Here, we attempted to present an optimized MII triple-clad optical fiber to obtain exciting performance in terms of dispersion and its slope [24]. The index refraction profile of the MII fiber structure is shown in Fig. 1. According to the LP approximation [26] to calculate the electrical field distribution, there are two regions of operation and the guided modes and propagating wave vectors can be obtained by using two determinants which are constructed by boundary conditions [27].

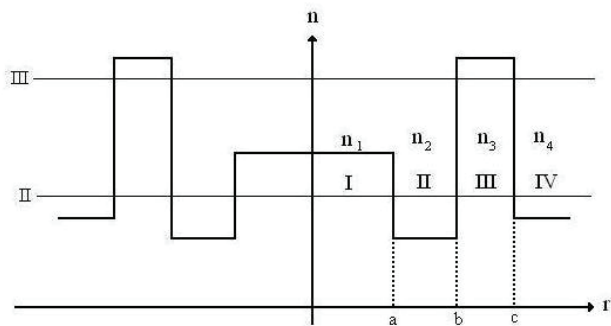


Fig. 1. Refractive index Profile for MII Structure.

For calculation of dispersion and dispersion slope the following parameters are used.

$$P = \frac{b}{c}, \tag{1}$$

$$Q = \frac{a}{c}, \tag{2}$$

where P and Q are geometrical parameters. Also, the optical parameters for the structure are defined as follows.

$$R_1 = \frac{n_3 - n_1}{n_3 - n_2}, \tag{3}$$

$$R_2 = \frac{n_2 - n_4}{n_3 - n_2}. \tag{4}$$

For evaluating of the index of refraction difference between core and cladding the following definition is done.

$$\Delta = \frac{n_3^2 - n_4^2}{2n_4^2} \approx \frac{n_3 - n_4}{n_4} \tag{5}$$

Here, we propose a novel methodology to make design procedure systematic. It is done by the aim of optimization technique and based on the Genetic Algorithm. A GA belongs to a class of evolutionary computation techniques [28] based on models of biological evolution. This method has been proved useful in the domains that are not understood well; search spaces that are too large to be searched efficiently through standard methods. Here, we concentrate on dispersion and dispersion slope simultaneously to achieve to the small dispersion and its slope in the predefined wavelength duration. Our goal is to propose a special fitness function that optimizes the pulse broadening factor. To achieve this, we have defined a weighted fitness function. In fact, the weighting function is necessary to describe the relative importance of each subset in the fitness function [24]; in other words, we let the pulse broadening factor have different coefficient in each wavelength. To weight the mentioned factor in the predefined wavelength interval, we have used the Gaussian weighting function. The central wavelength (λ_0) and the Gaussian parameter (σ) are used for the manipulation of the proposed fitness function and their effects on system dispersion and dispersion slope. To express the fiber optic structure, we considered three optical and geometrical parameters. According to the GA technique, the problem will have six genes, which explain those parameters. It should be mentioned that the initial range of parameters are chosen after some conceptual examinations. The initial population has 50 chromosomes, which cover the search space approximately. By using the initial population, the dispersion (β_2) and dispersion slope (β_3), which are the important parameters in the proposed fitness function, can be calculated. Consequently elites are selected to survive in the next generation. Gradually the fitness function leads to the minimum point of the search zone with an appropriate dispersion and slope. Equation (6) shows our proposal for the weighted fitness function of the pulse broadening factor.

$$F = \sum_{\lambda} e^{-\frac{(\lambda-\lambda_0)^2}{2\sigma^2}} \sum_Z [1 + (\frac{\beta_2(\lambda)Z}{t_i^2})^2 + (\frac{\beta_3(\lambda)Z}{2t_i^3})^2]^{\frac{1}{2}}, \quad (6)$$

where $\lambda_0, \sigma, t_i, Z, \beta_2$ and β_3 are central wavelength, Gaussian parameter, full width at half maximum, distance, second and third order derivatives of the wave vector respectively. In the defined fitness function in Eq. (6), internal summation is proposed to include optimum broadening factor for each length up to 200 km. By applying the fitness function and running the GA, the fitness function is minimized. So, the small dispersion and its slope are achieved. This condition corresponds to the maximum value for the dispersion length and higher-order dispersion length as well. By using this proposal, the zero dispersion wavelengths can be shifted to the central wavelength (λ_0). Since, the weight of the pulse broadening factor at λ_0 is greater than others in the weighted fitness function; it is more likely to find the zero dispersion wavelength at λ_0 compared to the other wavelengths. In the meantime, the flattening of the dispersion curve is controlled by Gaussian parameter (σ). To put it other ways, the weighting Gaussian function becomes broader in the predefined wavelength interval by increasing the Gaussian parameter (σ). As a result, the effect of the pulse broadening factor with greater value is regarded in different wavelengths, which causes a considerable decrease in the dispersion slope in the interval. Consequently, the zero dispersion wavelength and dispersion slope can be tuned by λ_0 and σ respectively. The advantage of this method is introducing two parameters (λ_0 and σ) instead of multi-designing parameters (optical and geometrical), which makes system design easy.

The flowchart given in Fig. 2 explains the foregoing design strategy clearly.

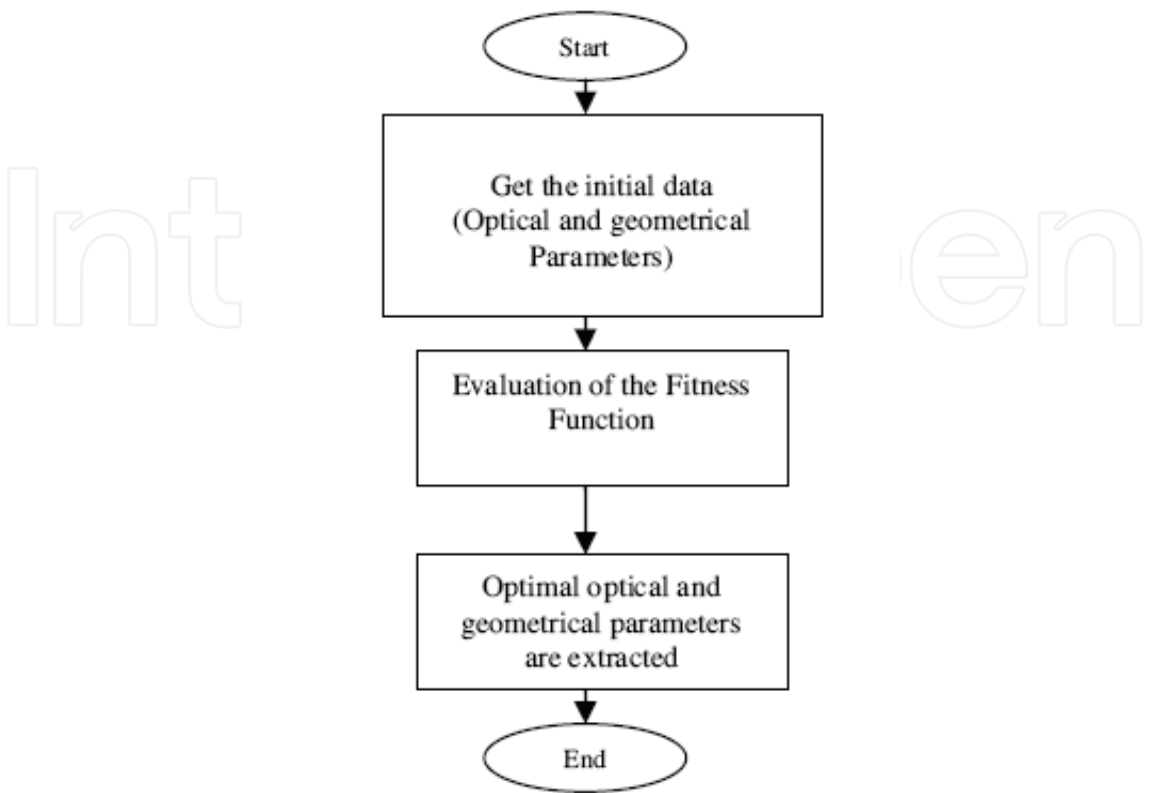


Fig. 2. The scheme of the design procedure

To illustrate capability of the suggested technique and weighted fitness function, the MII triple-clad optical fiber is studied, and the simulated results are demonstrated below. In the presented figures, we consider four simulation categories including dispersion related quantities, nonlinear behavior of the proposed fibers, electrical field distribution in the structures, and fiber losses.

For all the simulations, we consider $\lambda_0=1500, 1550\text{ nm}$ and $\sigma = 0, 0.027869$ and $0.036935\text{ }\mu\text{m}$ as design constants. To apply the GA for optimization, we consider the search space illustrated in Table 1 for each parameter as a gene. The choice of these intervals is done according to two items. The designed structure must be practical in terms of manufacturing and have high probability of supporting only one propagating mode [24].

Parameter	$a\text{ (}\mu\text{m)}$	p	Q	R_1	R_2	Δ
duration	[2-2.6]	[0.4-0.9]	[0.1-0.7]	[0.05-0.99]	[(-0.99)- (-0.05)]	[2×10^{-3} - 1×10^{-2}]

Table 1. Optimization Search Space of Optical and Geometrical Parameters

The wavelength and distance durations for optimization are selected as follows. For $\lambda_0=1550\text{nm}$: $1500\text{ nm}<\lambda<1600\text{ nm}$, for $\lambda_0=1500\text{ nm}$: $1450\text{ nm}<\lambda<1550\text{ nm}$, and $0<Z<200\text{ km}$. In this design method Z is variable. In the simulations an un-chirped initial pulse with 5 ps as full width at half maximum is used. Considering the information in Table 1 and GA method, optimal parameters are extracted and demonstrated in Table 2.

	λ_0 (μm)	a (μm)	Δ	R_1	R_2	p	Q
$\sigma=0$	1.55	2.0883	8.042e-3	0.5761	-0.4212	0.7116	0.3070
	1.5	2.1109	7.036e-3	0.6758	-0.2785	0.8356	0.2389
$\sigma = 2.7869 \times 10^{-8}$	1.55	2.0592	9.899e-3	0.7320	-0.2670	0.7552	0.2599
	1.5	2.5822	9.111e-3	0.5457	-0.4237	0.7425	0.2880
$\sigma = 3.6935 \times 10^{-8}$	1.55	2.2753	9.933e-3	0.5779	-0.4218	0.6666	0.3428
	1.5	2.5203	9.965e-3	0.4867	-0.3841	0.6819	0.3324

Table 2. Optimized Optical and Geometrical Parameters at $\lambda_0=1500, 1550$ nm and three given Gaussian parameters

It is found that optimization method for precise tuning of the zero dispersion wavelengths as well as the small dispersion slope requires large value for the index of refraction difference (Δ). That is to say that providing large index of refraction is excellent for the simultaneous optimization of zero dispersion wavelength and dispersion slope. First, we consider the dispersion behavior of the structures. To demonstrate the capability of the proposed algorithm for the assumed data, the obtained dispersion characteristics of the structures are illustrated in Fig. 3. It shows that the zero dispersion wavelengths can be controlled precisely by controlling the central wavelength. Meanwhile, the Gaussian parameters are used to manipulate the dispersion slope of the profile. Considering Fig. 3 and Table 3, it is found that the zero value for the Gaussian parameter can tune the zero dispersion wavelengths accurately (~ 100 times better than other cases).

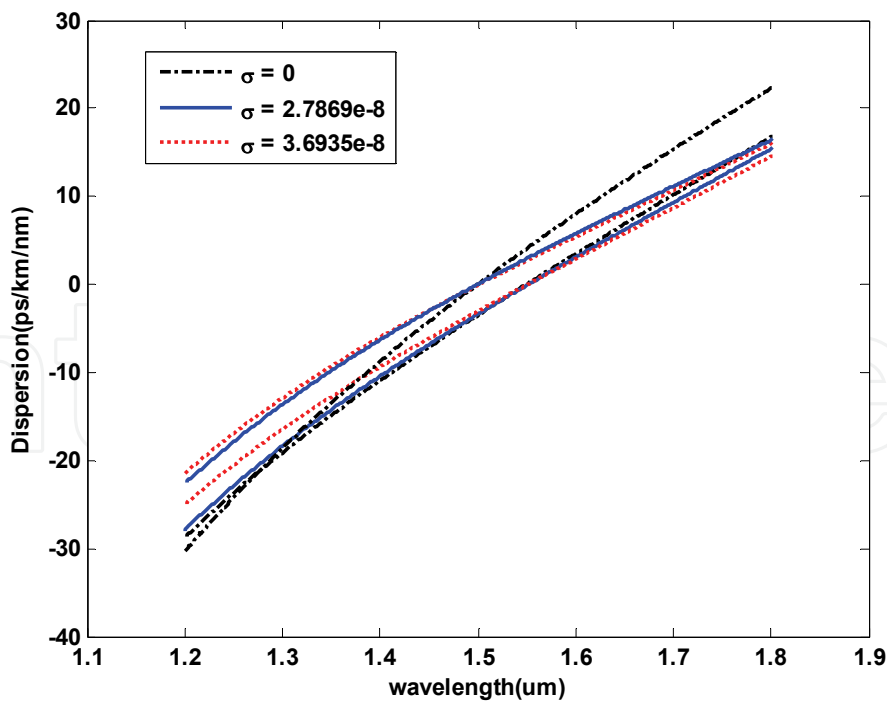


Fig. 3. Dispersion vs. Wavelength at $\lambda_0=1500\text{nm}, 1550\text{nm}$ with σ as parameter.

Second, the dispersion slope is examined. The presented curves say that by increasing the Gaussian parameter the dispersion slope becomes smaller, and it is going to be smooth in

large wavelengths. Furthermore it is clear that there is a trade-off between tuning the zero dispersion wavelengths and decreasing the dispersion slope as shown in Figs. 3, 4, and Table 3.

type	$\lambda_0(\mu m)$	Dispersion (ps / km / nm)	Dispersion Slope (ps / km / nm ²)	Effective Area (μm^2)	Mode Field Diameter (μm)	Quality Factor
$\sigma = 0$	1.55	-2.57e-4	0.0695	191.92	7.95	3.04
	1.5	2.55e-5	0.0828	344.15	9.76	3.61
$\sigma = 2.7869 \times 10^{-8}$	1.55	-0.013	0.0647	194.79	7.12	3.85
	1.5	0.008	0.0597	209.95	6.70	4.68
$\sigma = 3.6935 \times 10^{-8}$	1.55	-0.085	0.0592	150.05	6.82	3.22
	1.5	-0.089	0.0564	164.21	6.55	3.82

Table 3. Dispersion, Dispersion Slope, Effective Area, Mode Field Diameter and Quality Factor at λ_0 =1500nm, 1550nm and three given Gaussian parameters

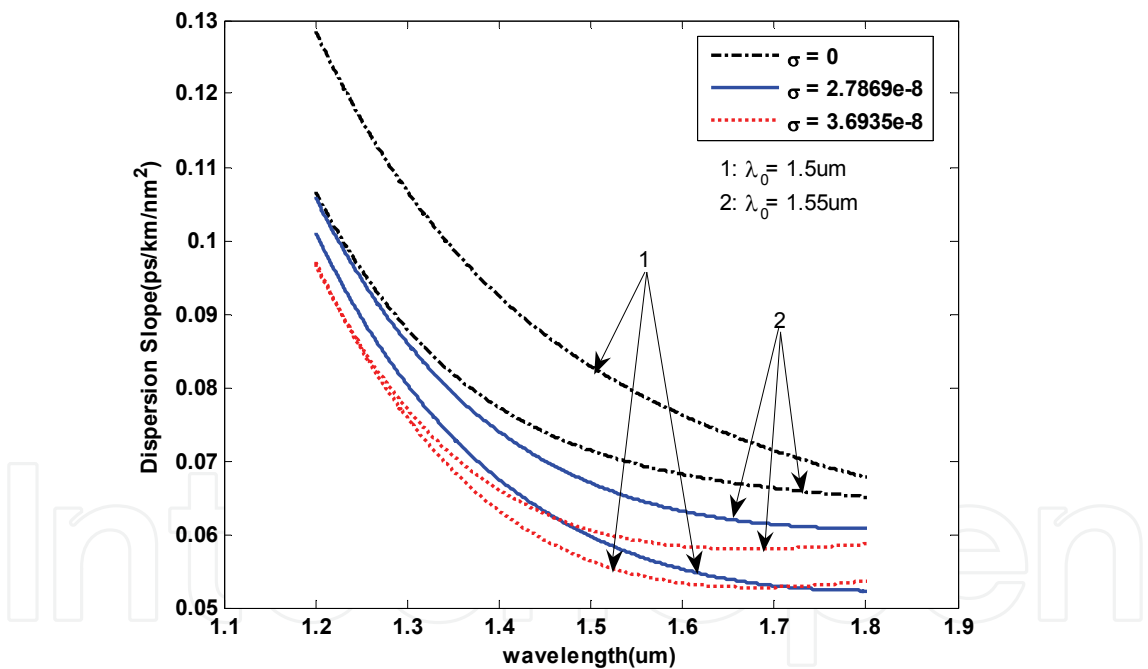


Fig. 4. Dispersion slope Vs. Wavelength at λ_0 =1500nm, 1550nm with σ as parameter.

The normalized field distribution of the MII based designed structures is illustrated in Figs. 5 and 6. Because of the special structure, the field distribution peak has fallen in region III. As such most of the field distribution displaces to the cladding region. In addition it is observed that the field distribution peak is shifted toward the core, and its tail is depressed in the cladding region by increasing the Gaussian parameter (except $\sigma=0$). On the other hand the field distribution slope increases inside the cladding region by increasing of the Gaussian parameter.

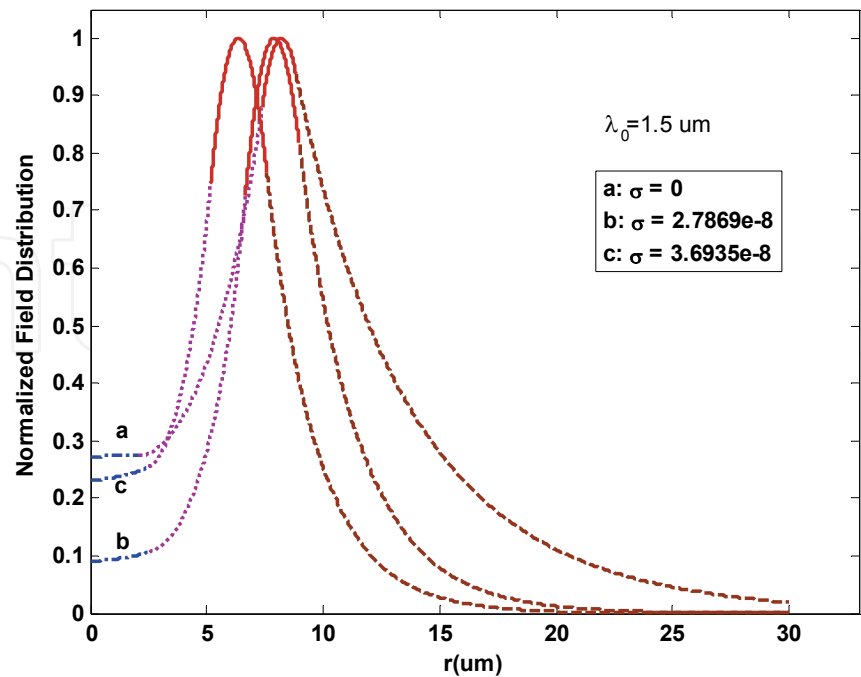


Fig. 5. Normalized Field distribution versus the radius of the fiber at $\lambda_0=1500\text{nm}$ with σ as parameter (dashed-dotted, dotted, solid line, and dashed curves represent regions I, II, III and IV respectively).

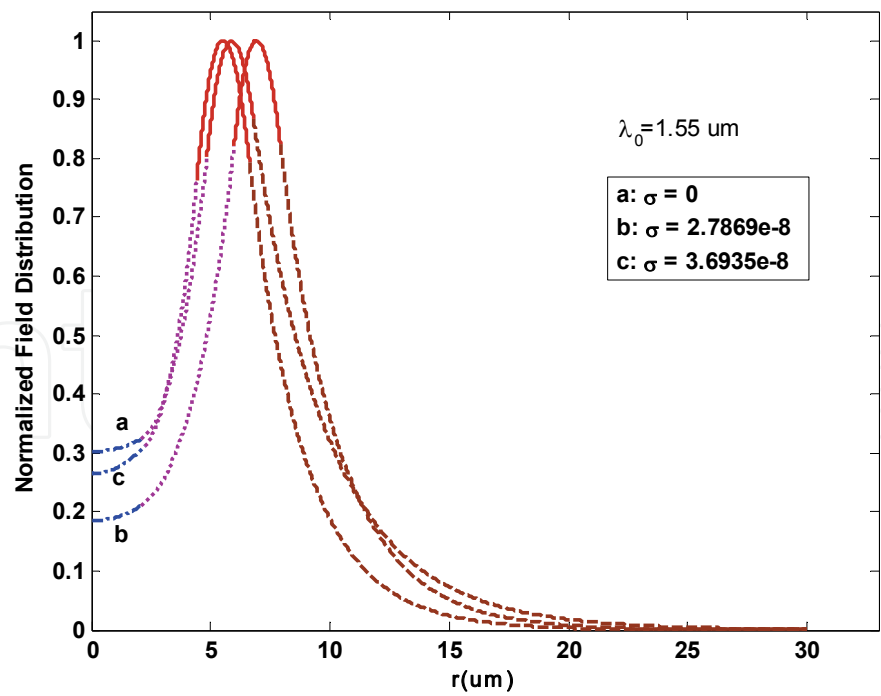


Fig. 6. Normalized Field distribution versus the radius of the fiber at $\lambda_0=1550\text{nm}$ with σ as parameter (dashed-dotted, dotted, solid line, and dashed curves represent regions I, II, III and IV respectively).

The effective area or nonlinear behavior of the suggested structures is illustrated in Fig. 7. It is observed that the effective area becomes smaller by increasing the Gaussian parameter. Figs. 5–7, and Table 3 indicate a trade-off between the large effective area and the small dispersion slope. The results illustrated in Fig. 4 show that the dispersion slope reduces by increasing the Gaussian parameter. However the field distribution shifts toward the core, which concludes the small effective area in this case. Foregoing points show that there is an inherent trade-off between these two important quantities.

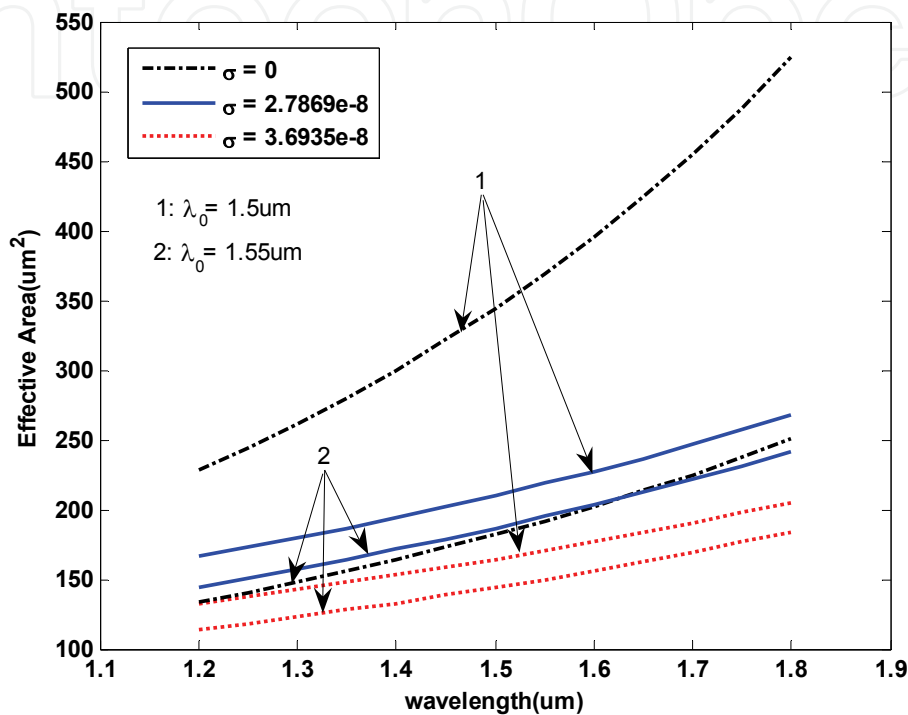


Fig. 7. Effective area versus wavelength at $\lambda_0=1550\text{nm}$, 1500nm with σ as the parameter.

The mode field diameter that corresponds to the bend loss is illustrated in Figs. 8 and 9 for both central wavelengths. It is clearly observed that the mode field diameter decreases by increasing the Gaussian parameter. In other words, the Gaussian parameter is suitable for the bend loss manipulation in these structures. Furthermore, Table 3 shows that the mode field diameter is $\sim 7\mu\text{m}$ in the designed structure.

As another concept to consider, Table 3 says that the mode field diameter is not affected noticeably by increasing the effective area. This is the origin of raising the quality factor in these structures. This is a key point why the average amount of the quality factor in the proposed structures is increased in Fig. 9. The quality factor of the designed fibers is illustrated in Fig. 10. The calculations show that the quality factor is generally larger than 3. It is mentionable that the quality factor is smaller than unity in the inner depressed clad fibers (*W* structures) and around unity in the depressed core fibers (*R* structures). This feature shows the high quality of the putting forward methodology. It is observed that the quality factor decreases by increasing the Gaussian parameter. It is strongly related to the effective area reduction.

As another result the dispersion length is illustrated in Fig. 11 for the given Gaussian parameter and two central wavelengths. The narrow peaks at $\lambda=1500\text{nm}$ and 1550nm imply

the precise tuning of the zero dispersion wavelengths. The higher-order dispersion length of the designed fibers is demonstrated in Fig. 12. It is clear that the higher-order dispersion length increases by raising the Gaussian parameter.

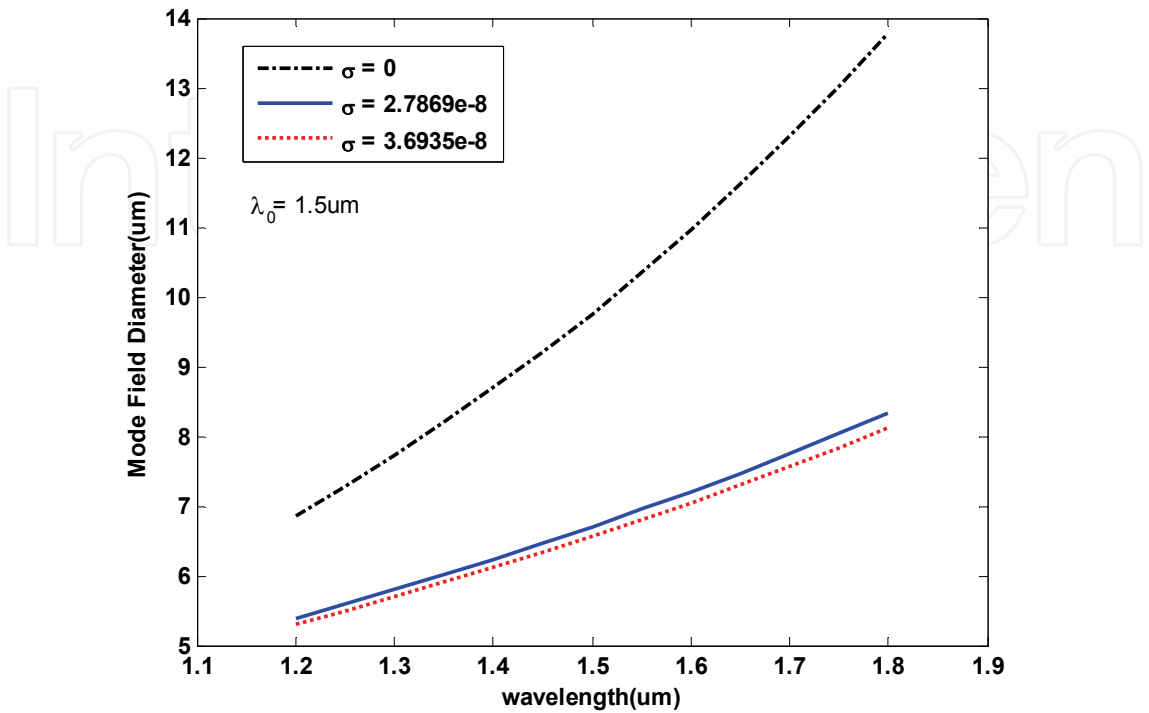


Fig. 8. Mode Field Diameter versus wavelength at $\lambda_0=1500\text{nm}$ with σ as parameter.

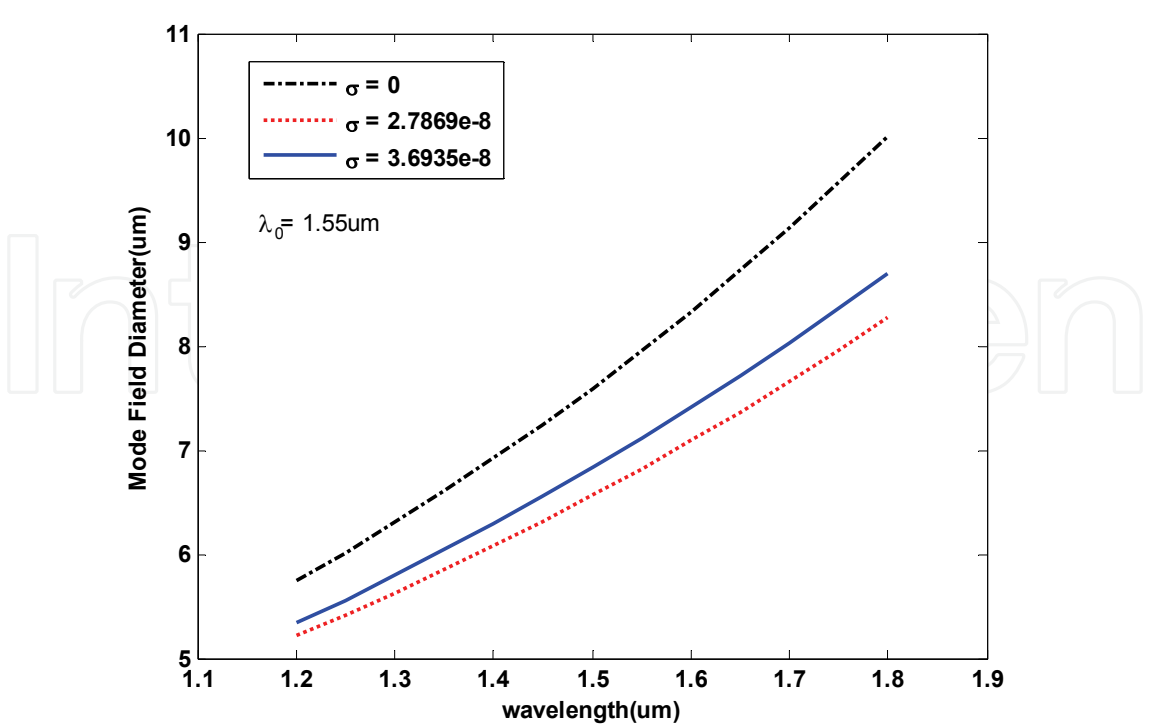


Fig. 9. Mode Field Diameter versus wavelength at $\lambda_0=1550\text{nm}$ with σ as parameter.

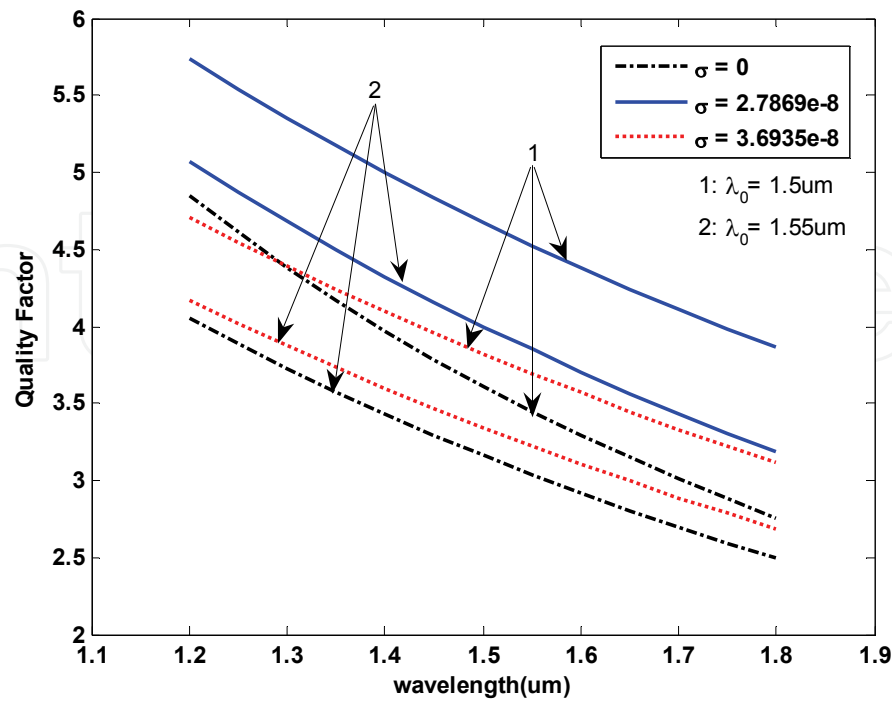


Fig. 10. Quality Factor versus wavelength at $\lambda_0=1500\text{nm}$, 1550nm with σ as parameter.

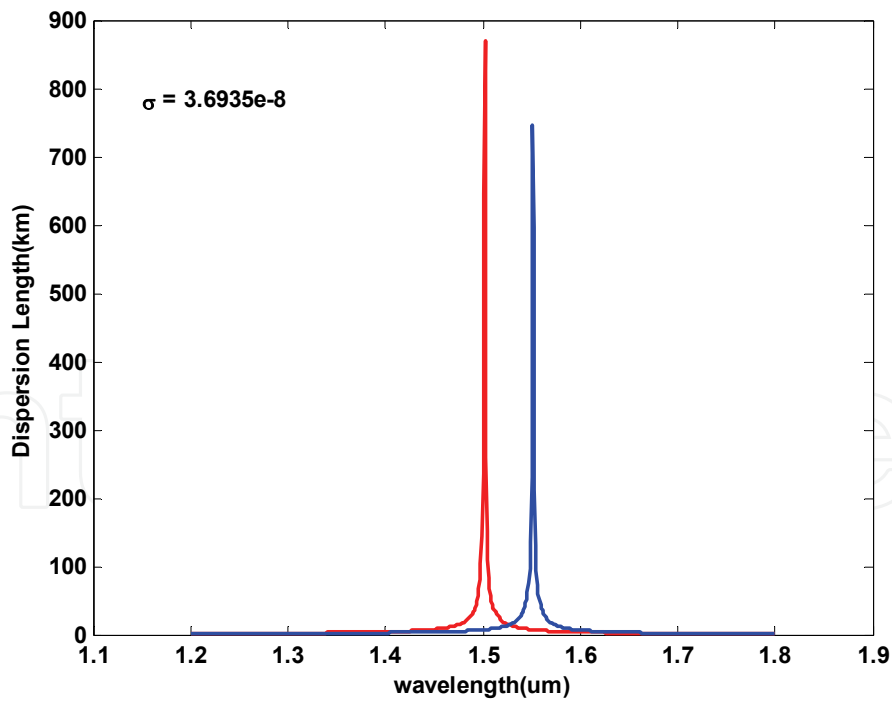


Fig. 11. Dispersion Length vs. Wavelength at $\lambda_0 = 1.5, 1.55 \mu\text{m}$.

In the following, the nonlinear effect length for 1 mW input power is illustrated in Fig. 13. First, it can be extracted that the suggested structures have the high nonlinear effect length. For the general distances, these simulations show that the fiber input power can become some hundred times greater to have the nonlinear effect length comparable with the fiber

dispersion length. Second, the nonlinear effect length decreases and increases, respectively, by raising the Gaussian parameter and wavelength.

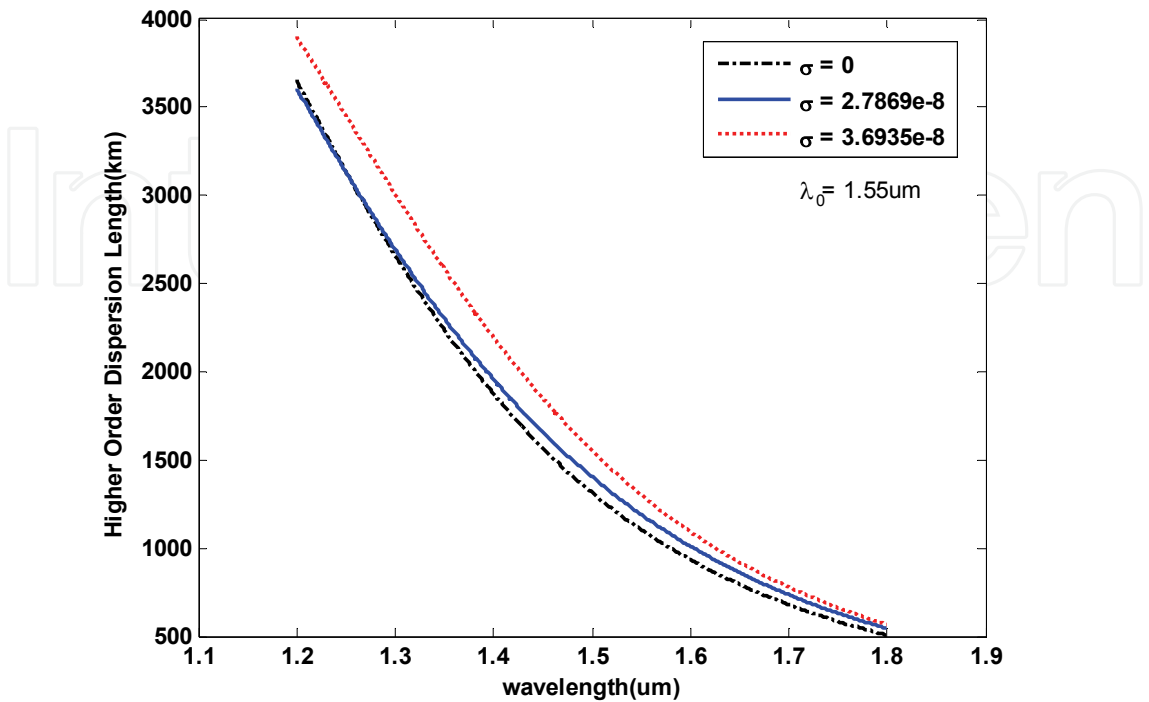


Fig. 12. Higher Order Dispersion Length vs. Wavelength at $\lambda_0 = 1.55 \mu m$ and Variance of the weight function as parameter.

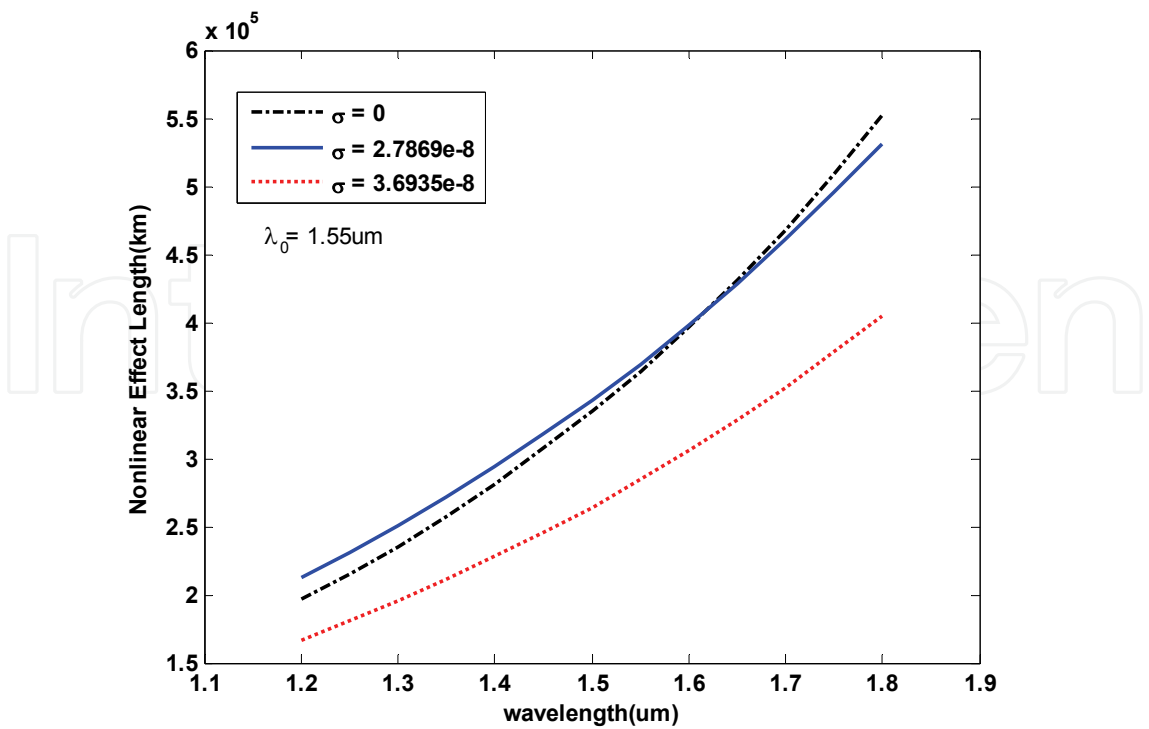


Fig. 13. Nonlinear Effective Length versus wavelength at $\lambda_0 = 1550 \text{ nm}$ with σ as parameter.

The amount of the fiber bending loss strongly depends on the bend radius and the mode field diameter. Figures 14 and 15, respectively, illustrate the bending loss (dB/m) versus the bending radius (mm) at $\lambda_0= 1550\text{ nm}$ and 1500nm with variance of the weighting function (σ) as a parameter. According to Figs. 8, 9, 14, and 15, it is clear that smaller mode field diameter yields to the greater tolerance to the bending loss.

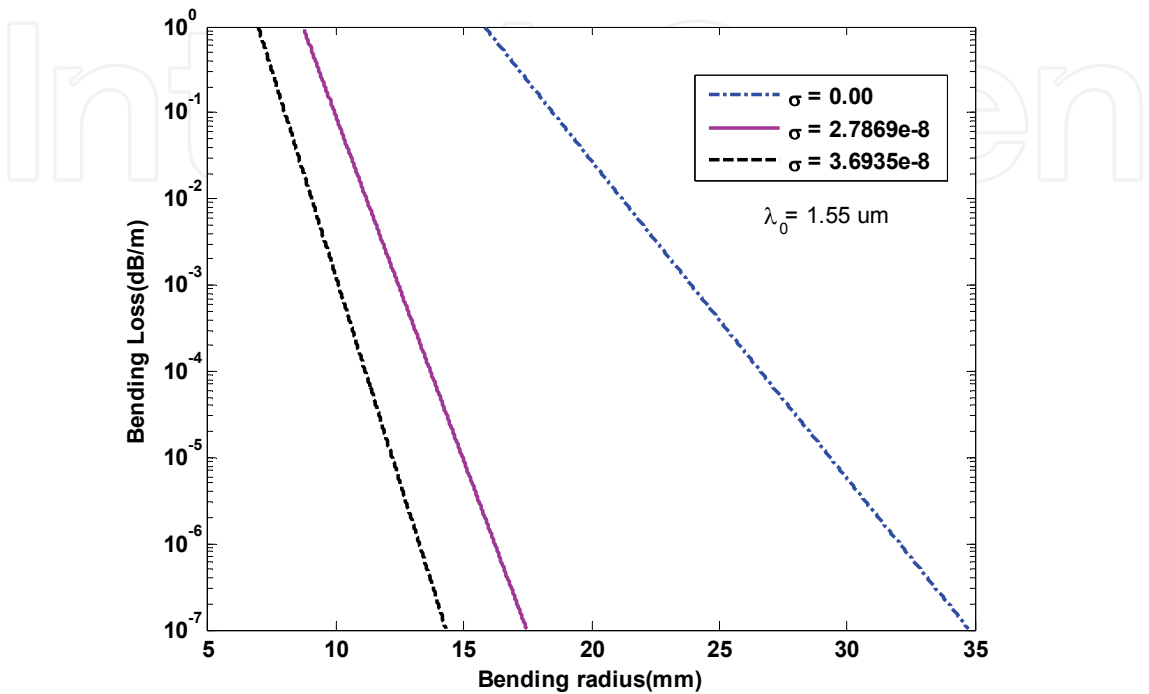


Fig. 14. Bending loss (dB/m) Vs. Bending radius at $\lambda_0=1550\text{nm}$ with σ as parameter.

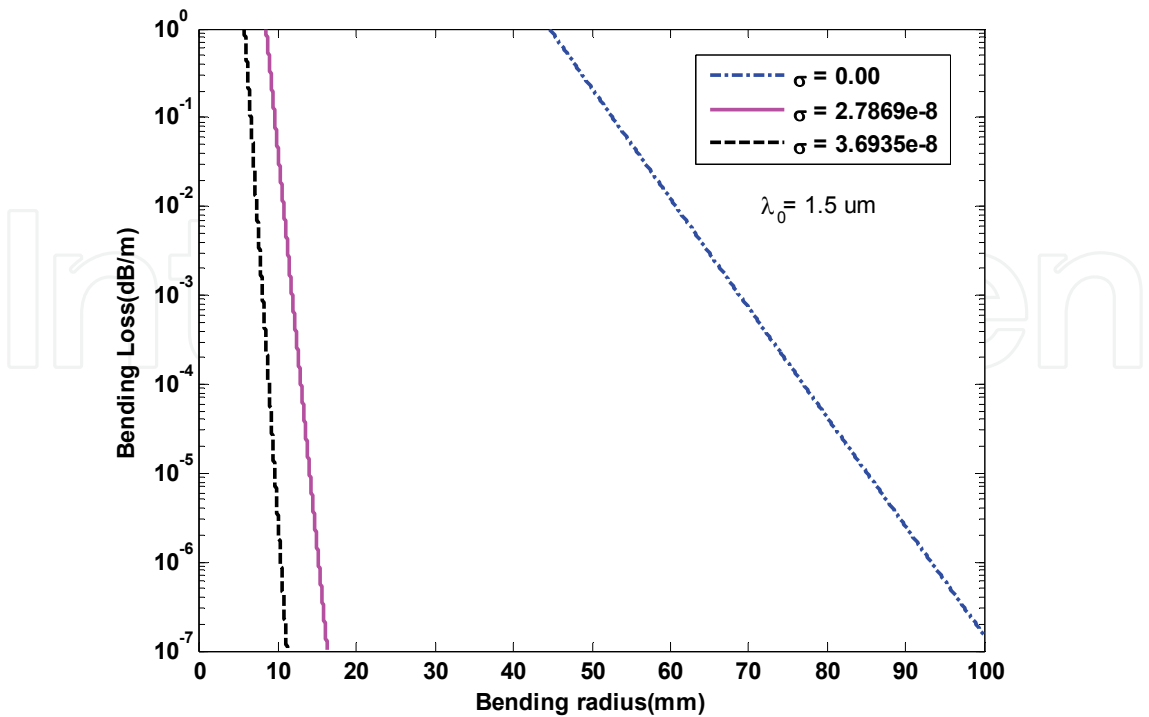


Fig. 15. Bending loss (dB/m) Vs. Bending radius at $\lambda_0=1500\text{nm}$ with σ as parameter.

All of the presented outcomes show that the suggested idea has capability to introduce a fiber including higher performance. We have presented a novel method that includes the small dispersion, its slope, high effective area, and small mode field diameter simultaneously [24]. So all options required for the zero dispersion shifted communication system are achieved successfully. This advantage is obtained owing to the selection of the basic fiber structure as well as the method of optimization. Our selected fiber structure is the MII, and we use the weighted fitness function applied in the GA for optimization. By combining the suitable structure and the novel optimization method, all of the stated advantages can be gathered simultaneously. The features of the proposed method are capable of being extended to all of fiber structures, introduce two parameters instead of multi-designing parameters, and tune the zero dispersion wavelengths precisely.

The ring index profiles fibers have been closely paid attentions because it has the larger effective-areas that can minimize the harmful effects of fiber nonlinearity [29]. For the proposed MII fiber structures, the small dispersion and its slope have been obtained thanks to a design method based on genetic algorithm. But there is not any concentration on the bending loss characteristic at the design process. Here we want to enter bending loss effect on the fitness function directly and attempt to present an optimized RII triple-clad optical fiber to obtain the wondering performance from dispersion, its slope, and bending loss points of view. The index refraction profile of the RII fiber structure is shown in Fig. 16.

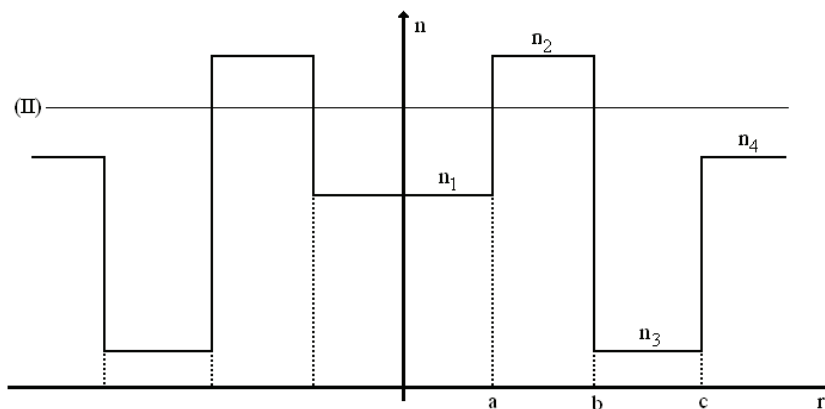


Fig. 16. Index of Refraction Profile for RII Structure

To calculate the dispersion, its slope and bending loss characteristics of the structure, the geometrical and optical parameters are defined as follows.

$$P = \frac{b}{c}, \quad Q = \frac{a}{c} \quad (7)$$

$$R_1 = \frac{n_2 - n_3}{n_2 - n_1}, \quad R_2 = \frac{n_1 - n_4}{n_2 - n_1}, \quad \Delta = \frac{n_2^2 - n_4^2}{2n_4^2} \approx \frac{n_2 - n_4}{n_4}. \quad (8)$$

The design method is based on the combination of the Genetic Algorithm (GA) and Coordinate Descent (CD) approaches. It is well known that the GA is the scatter-shot and the CD is the single-shot searching technique. The single-shot search is very quick compared to the scatter-shot type, but depends critically on the guessed initial parameter values. This description indicates that for the CD search, there is a considerable emphasis on the initial search position. In this method, it is possible to define a fitness function and evaluate every

individuals of the population with it. So we have combined the CD and GA methods to improve the initial point selection with the help of generation elite and inherit the quick convergence of coordinate descent [30]. In other words, we cover and evaluate the answer zone by initial population and deriving few generations and use the elite of the latest generation as an initial search position in the CD (Fig. 17).

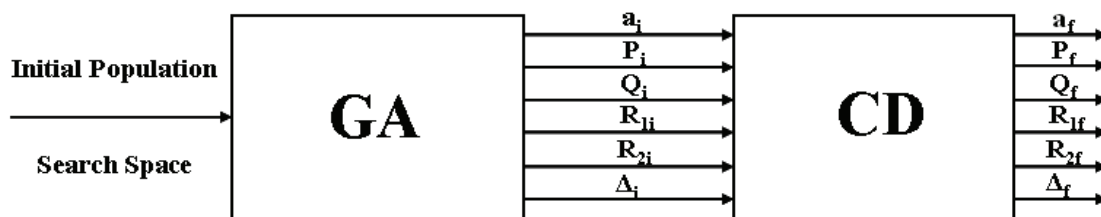


Fig. 17. The Block Diagram of The Proposed Method

To derive the suggested design methodology, the following weighted cost function is introduced. We have normalized the pulse broadening factor in the manner to be comparable with bending loss. This normalization is essential to optimize the pulse broadening factor and bending loss simultaneously. If not, the bending loss impact will be imperceptible and be lost in the broadening factor term.

$$F = \sum_{\lambda} e^{-\frac{(\lambda - \lambda_0)^2}{2\sigma^2}} \left(\frac{1}{Z} \sum_Z \left[\left(1 + \frac{\beta_2(\lambda)Z}{t_i^2} \right)^2 + \left(\frac{\beta_2(\lambda)Z}{t_i^2} \right)^2 + \left(\frac{\beta_3(\lambda)Z}{2t_i^3} \right)^2 \right]^{\frac{1}{2}} \right) + BL(\lambda), \quad (9)$$

The bending radius is set on 1 cm and kept still. The fitness function includes dispersion (β_2), dispersion slope (β_3), and bending loss (BL) impacts. In the defined weighted fitness function, internal summation is proposed to include optimum broadening factor for each length up to 200 km. as said at the beginning of this section, one can adjust the zero dispersion wavelength at λ_0 and dominate the dispersion slope by Gaussian parameter (σ). The obtained dispersion behaviors of the structures are illustrated in Fig. 18 which obviously demonstrates the λ_0 and σ parameters influences. It is clear that the zero-dispersion wavelength is successfully set on λ_0 and the dispersion curve is become flatter in the higher σ cases.

To show the capability of the proposed algorithm, Table 4 is presented to clarify the different characteristics of these three structures. By considering on Fig. 18 and Table 4, it is clear that there is a trade-off between the zero dispersion wavelength tuning and the dispersion slope decreasing. In other words, it is found out that the zero value for the σ parameter can tune the zero dispersion wavelength accurately (~100 times better than other cases).

The effective area or nonlinear behavior of the suggested structures is listed in Table 4. These values are high enough for the optical transmission applications. Owing to the special structure of the RII type fiber, the field distribution peak has fallen in the first cladding layer. As such most of the field distribution displaces to the cladding region. This is the origin of large effective area in the designed structures. The normalized field distribution of the RII based designed structures is illustrated in Fig. 19.

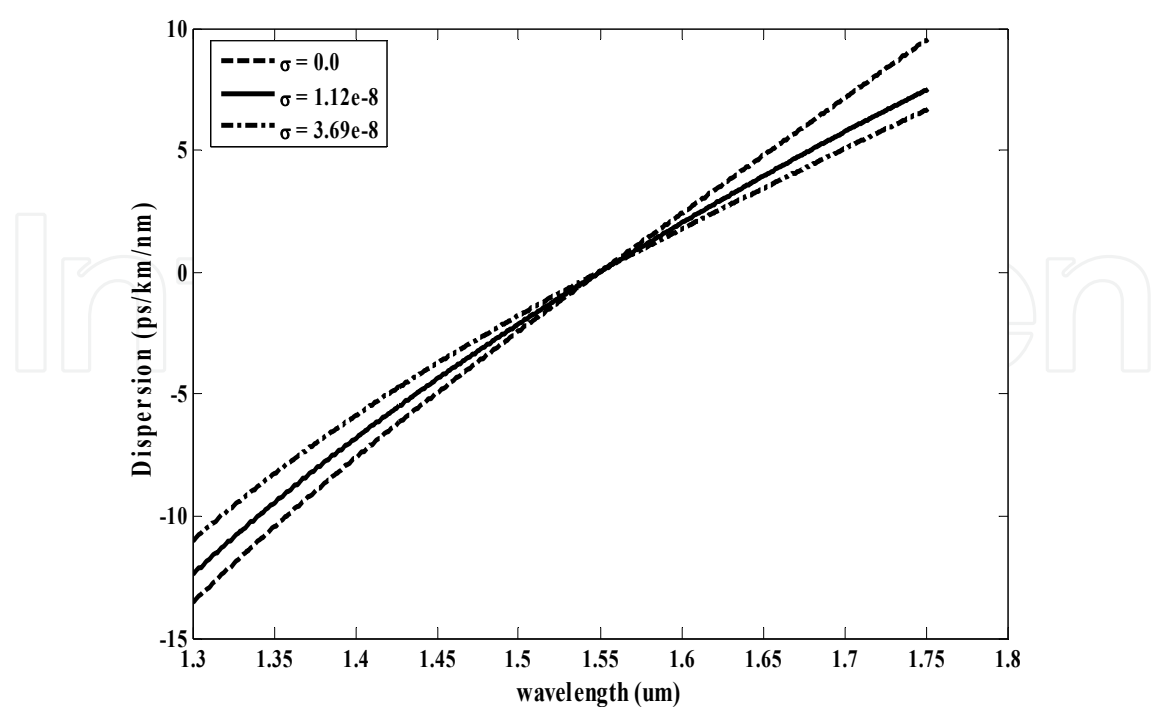


Fig. 18. Dispersion vs. Wavelength at $\lambda_0=1.55\text{ }\mu\text{m}$.

type	$D(\lambda=1.55\text{ }\mu\text{m})$ (ps/km/nm)	$S(\lambda=1.55\text{ }\mu\text{m})$ (ps/km/nm ²)	$BL(\lambda=1.55\text{ }\mu\text{m})$ (dB/m)	$A_{eff}(\lambda=1.55\text{ }\mu\text{m})$ (μm^2)
$\sigma = 0.0$	1.38e-4	0.048	1.90e-2	86.84
$\sigma = 1.12\text{e-}8$	-6.15e-4	0.041	1.67e-1	82.53
$\sigma = 3.69\text{e-}8$	4.50e-2	0.035	4.66e-2	86.01

Table 4. Dispersion, Dispersion Slope, Bending Loss, and Affective Area at $\lambda_0=1.55\text{ }\mu\text{m}$ and Three Given Gaussian Parameters

Due to the refractive index thermo-optic coefficient and the thermal expansion coefficient, the optical and geometrical parameters are altered. Consequently, the optical transmission characteristics of the optical fiber such as dispersion, its slope and bending loss are confronted to change. In order to evaluate the thermal stability of the designed structures, the following results are extracted and presented in Table 5. The dD/dT , dS/dT , $d\lambda_0/dT$, and dBL/dT expressions are respectively the chromatic dispersion, its slope, zero dispersion wavelength, and bending loss thermal coefficients at $1.55\mu\text{m}$. It is found out that this environmental factor must be considered in the desired optical fiber design. For example, in the worst case, the zero dispersion wavelengths can be shifted more than 3 nm with 100°C . In the least design we have focused on RII depressed core triple clad single mode optical fiber and presented a combined optimization approach to obtain desirable design goals. Furthermore, we have used the special fitness function including dispersion, its slope and bending loss impacts simultaneously. With application of this fitness function in the case of higher σ , we could obtain the dispersion and dispersion slope in [1.5 - 1.6] μm interval to be

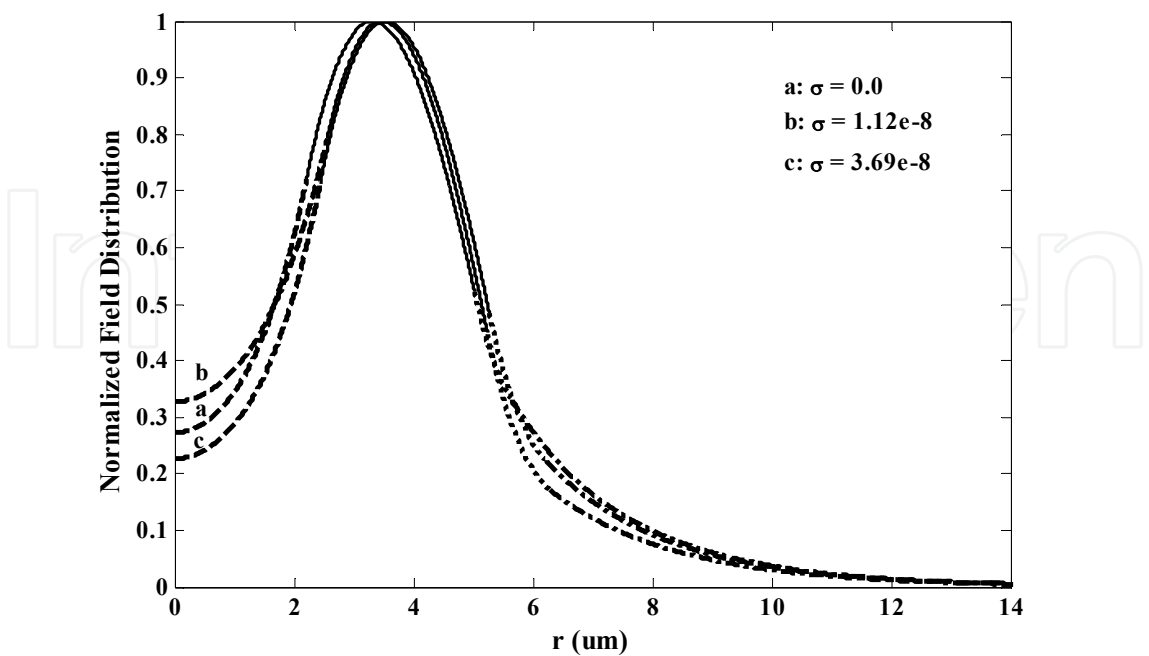


Fig. 19. Normalized field distribution versus the radius of the fiber at $\lambda=1.55\text{ }\mu\text{m}$ with σ as parameter (dashed, solid line, dotted, and dashed-dotted curve represent the core and three cladding layers, respectively).

Type	$\frac{dD}{dT}$ (ps/km/nm/°C)	$\frac{dS}{dT}$ (ps/km/nm ² /°C)	$\frac{d\lambda_0}{dT}$ (nm/°C)	$\frac{dBL}{dT}$ (dBL/m/°C)
$\sigma = 0.0$	-1.22×10^{-3}	$+2.83\times 10^{-6}$	$+2.5\times 10^{-2}$	$+3.97\times 10^{-6}$
$\sigma = 1.12\text{e-}8$	-1.21×10^{-3}	$+2.93\times 10^{-6}$	$+3.33\times 10^{-2}$	$+2.70\times 10^{-5}$
$\sigma = 3.69\text{e-}8$	-1.21×10^{-3}	$+2.93\times 10^{-6}$	$+2.5\times 10^{-2}$	$+8.79\times 10^{-6}$

Table 5. Dispersion, Dispersion Slope, and Bending Loss Thermal Coefficients at $\lambda_0=1.55\text{ }\mu\text{m}$ and Three Given Gaussian Parameters [(-1.77) - (+1.77)] ps/km/nm and [(0.037) - (0.033)] ps/km/nm². Also the amount of bending loss at 1.55 μm with 1cm radius of curvature and effective area are 4.66e-2 dB/m and 86.01 μm^2 respectively. In the meantime, the thermal stabilities of the designed structures are evaluated. It is possible to design zero dispersion shifted by using graded index structure. The main options are dispersion value and the effective area at 1550nm to minimize pulse broadening and nonlinearity effects. Excess investigation of large mode area fibers show that there is not serious focusing on design of zero dispersion shifted fiber based on the graded index refractive structures. The index refraction profile of the triangular-core graded index optical fiber structure, which is suggested by us for the first time, is shown in Fig. 20. It is clear that the proposed graded index fiber has a linear variation in core region. According to the TMM approach, it is assumed that the refractive index of the fiber with an arbitrary but axially symmetric profile is approximately expressed by a staircase function. So the field distribution and guided modes are calculated [26].

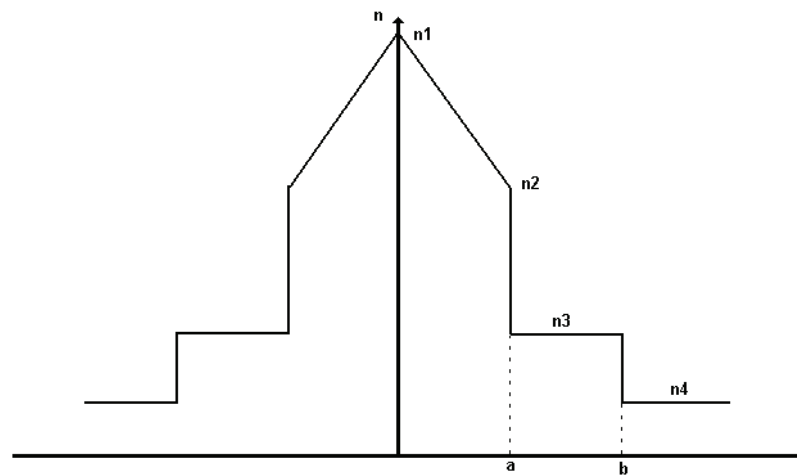


Fig. 20. Refractive Index Profile for Triangular Core Graded Index Fiber Structure

Also for easy handling of the problem and calculating the dispersion and its slope of the proposed fiber, following optical and geometrical parameters are defined.

$$\Delta = \frac{n_1^2 - n_4^2}{2n_4^2} \approx \frac{n_1 - n_4}{n_4}, \quad P = \frac{a}{b}, \quad n_3 = n_4 + \eta(n_2 - n_4), \quad n_2 = n_3 + \mu(n_1 - n_3). \quad (9)$$

In order to explain layers' refractive index, η and μ coefficients are introduced and set between 0 and 1. It must be declared that P parameter relates the cladding layer thickness with the core radius. The design method is based on the limited coordinate descent (CD) approach [30]. Based on the extensive investigation, it is found out that the smaller core radius and larger refractive index difference lead the zero dispersion wavelength to around $1.55\mu\text{m}$. Therefore in order to design the dispersion shifted optical fiber, Δ and core radius are set to 8×10^{-3} and $1.8\mu\text{m}$ respectively. Also it is assumed that the core and first cladding layer have same thickness. Then direct search is done for η and μ parameters in the $[0,1]$ interval. To derive the suggested design methodology, the following fitness function is introduced which includes the pulse broadening factor.

$$F = \sum_Z \left[\left(1 + \frac{\beta_2(\lambda_0)Z}{t_i^2} \right)^2 + \left(\frac{\beta_2(\lambda_0)Z}{t_i^2} \right)^2 + \left(\frac{\beta_3(\lambda_0)Z}{2t_i^3} \right)^2 \right]^{\frac{1}{2}} \quad (10)$$

In the defined fitness function, the summation is proposed to include optimum broadening factor for each length up to 200 km. The short glance on eq.(10) shows that the above fitness function is a limited version of the past one [24], which the wavelength duration optimizing is abbreviated. Also, it is not weighted because the fitness function is evaluated at single wavelength (λ_0). One can adjust the zero dispersion wavelength at λ_0 . It should be kept in mind that in the fiber design, one likes to shift the zero dispersion wavelength to the region that the fiber has the lowest level attenuation. The optical attenuation has a global minimum around $1.55\mu\text{m}$ wavelength and that is why the most optical communication systems are operated at this wavelength. Seeing that, the λ_0 parameter of the applied method is set to $1.55\mu\text{m}$ to achieve the desired zero dispersion shifted structure. Considering the parameter presented above and CD method, the design procedure is driven and optimal parameters are extracted and demonstrated in Table 6.

Core radius	Δ	p	η	μ
*1.8 μm	8×10^{-3}	0.5	0.25	0.44

*b=2a

Table 6. The Optical and Geometrical Parameters for the Designed Structure.

The value of the dispersion is -0.04549ps/km/nm at 1.55 μm , which is properly small. The nonlinear effects in a single mode fiber are the ultimate restricting factors for bit rate and distance in long haul optical fiber communication system. Therefore, the large effective area single mode fibers have been the subject of considerable studies recently. The effective area of the suggested structure is 65.3 μm^2 at 1.55 μm , which is acceptable for this application. The associated mode field diameter at aforesaid wavelength is 9.03 μm .

8. Non-Zero Dispersion Shifted Fibers (NZDSFs)

Use of commercially available erbium doped fiber amplifiers (EDFA), which forces optical communication systems to be operated in the 1550 nm window, has significantly reduced the link length limitation imposed by attenuation in the optical fiber. However, high bit rate (~ 10 Gb/s) data transmission can be limited by the large inherent dispersion of the fiber. Dispersion shifted fibers (DSF), which has zero dispersion around 1550 nm, have been proposed and developed to overcome this problem. However in order to increase the information carrying capacity, latest high speed communication system is based on the dense wavelength division multiplexing/demultiplexing (DWDM). In such systems, nonlinear effects like four wave mixing (FWM), which arise due to simultaneous transmission at many closely spaced wavelengths and high optical gain from EDFA, imposes serious limitations on the use of a DSF with zero dispersion wavelength at 1550 nm. To overcome this difficulty, the nonzero dispersion shifted fibers having small dispersion in the range ~ 2-4 ps/km/nm over the entire gain window of EDFA have been proposed. In such fibers, the phase matching condition is not satisfied and hence the effect of FWM becomes negligible due to small dispersion. Nonlinear effects like cross phase modulation (XPM), which limits the numbers of different wavelength signals, can be reduced by increasing the mode field diameter (MFD) and hence effective area of the fiber. Therefore large effective area nonzero dispersion shifted fibers have been developed [31]. To achieve large effective area and low bending and splice loss with conventional fiber, a refractive index profile, as shown in Fig. 21, is designed, which is mathematically described by Eq. (11).

$$\left\{ \begin{array}{ll} n_1 & |r| \leq R_1 \\ n_1 \sqrt{1 - 2\Delta_1 \left(\frac{r-R_1}{R_2-R_1} \right)^{\alpha}} & R_1 < |r| \leq R_2 \\ n_2 & R_2 < |r| \leq R_3 \\ n_3 \sqrt{1 - 2\Delta_2 \left(\frac{R_{34}-r}{R_{34}-R_3} \right)^{\alpha}} & R_3 < |r| \leq R_{34} \\ n_3 \sqrt{1 - 2\Delta_2 \left(\frac{r-R_{34}}{R_4-R_{34}} \right)^{\alpha}} & R_{34} < |r| \leq R_4 \\ n_2 & |r| > R_4 \end{array} \right. \tag{11}$$

where R_1, R_2, R_3, R_4 are radius parameters, $R_{34}=(R_3+R_4)/2$ is the center of the side core, n_1, n_2, n_3 are the highest refractive index of central core, refractive index of cladding, and highest refractive index of side core, respectively, $\Delta_1=(n_1-n_2)/n_2$ and $\Delta_2=(n_3-n_2)/n_2$ are the relative profile heights of central core and side core, respectively, and α is the curve parameter. This fiber consists of three parts, including a central core, side core and a cladding layer. The side core inside the core region (i.e., the region $r<R_4$) is designed to allow more signal energy to flow into the cladding region so that a large effective area can be obtained [31].

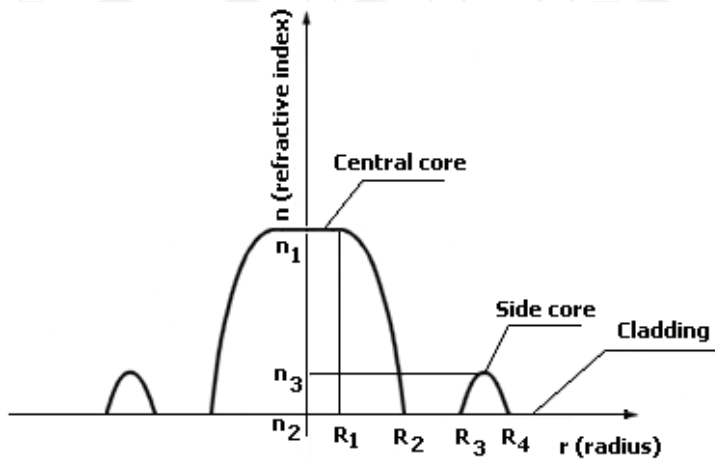


Fig. 21. Refractive index profile of newly designed large effective area, low bending and splice loss NZ-DSF.

From Eq. (11) it is found that the exact refractive index profile are controlled by seven parameters (i.e., $R_1, R_2, R_3, R_4, \Delta_1, \Delta_2$, and α). To ensure the single mode operation, $R4$ must be less than certain number. Thus, there are six parameters need to be optimized for achieving the required dispersion slope, large effective area, low splice loss, low bending loss, and low Rayleigh scattering loss simultaneously. By using the random searching method, it is found that the fiber has the optimum performance under the following conditions:

$$\left\{ \begin{array}{l} a = 3.2\mu\text{m (radius of fiber core)} \\ R_1 = 0.218309a = 0.6986\mu\text{m} \\ R_2 = 0.568242a = 1.8184\mu\text{m} \\ R_3 = 0.7325779a = 2.3442\mu\text{m} \\ R_4 = 1.0a = 3.2\mu\text{m} \\ \Delta_1 = 0.6425\% \\ \Delta_2 = 0.2378\% \\ \alpha = 1.6 \end{array} \right. \quad (12)$$

The Gaussian approximation method is used for calculating electrical field distribution for the designed refractive index profile. The designed fiber has a dispersion about 4 ps/km/nm and dispersion slope about 0.06 ps/km/nm² at 1.55 μm operating wavelength, which can be used to avoid four-wave mixing (FWM). Also the zero dispersion wavelength is adjusted near 1480nm. In addition, calculation also shown that the designed fiber not only has a large effective area over 100 μm^2 but also has low bending loss ($<1.3\times10^{-3}$ dB with 30 mm bending radius and 100 turns) and low splice loss ($<6.38\times10^{-3}$ dB) with conventional

fiber. In order to broaden the wavelength range – not only the conventional C-band (1530–1565 nm) – but also the L-band (1565–1620 nm) and S-band (1460–1530 nm), the dispersion slope should be as low as possible, which can decrease the cost of dispersion compensation and suppress the self-phase modulation, especially for the 40 Gb/s communication system. Now we present a new depressed core index dual ring profile, which can provide a large A_{eff} and a low dispersion slope simultaneously, and the zero dispersion wavelength is less than 1430 nm [32]. The fibers with this refractive index profile have the low bending loss and low intrinsic loss. The splice loss also can reach the accepted value as it is spliced with conventional single mode fiber. The principal design requirements for the fibers are large A_{eff} , small dispersion slope, low bending and intrinsic loss, low polarization-mode dispersion, and zero dispersion wavelength that should be lower than 1430 nm. Relative refractive index Δn_i is defined by the equation: $\Delta n_i=(n_i-n_c)/n_c$, where n_c is the outer cladding layer’s refractive index. The dopant in the glass can decrease the glass viscosity, i.e, more dopant concentration means less glass viscosity. High difference value between Δn_1 and Δn_2 may cause high difference value in viscosity property of the depressed core layer and the first raised ring. Therefore, more mechanical stress will be built in the optical fibers during the drawing process [33]. On the other hand, high difference value between layers’ refractive index can increase the compositional variation in the optical fiber. Therefore, more thermal stress can be also caused by the radial variation of thermal expansion coefficient due to the big compositional variation in optical fiber [34]. The residual stress in optical fibers can not only weaken the strength of optical fibers, but also increase the fiber’s attenuation and polarization mode dispersion values. According to the above description, the refractive index profile shown in figure 22 is proposed to overcome problems. Every parameters of the fiber profile are set out in Table 6, where Δn_i are the relative refractive index of different layer from the depressed core layer to the cladding, respectively.

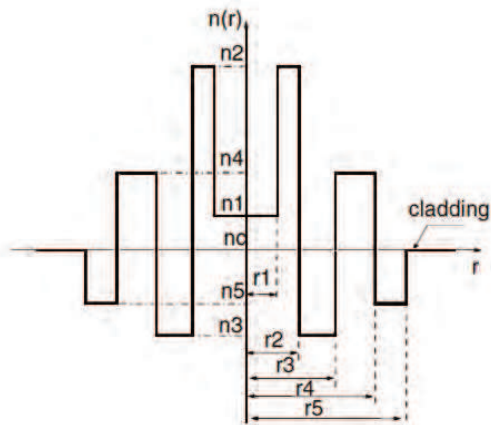


Fig. 22. Improved refractive index profile with dual ring and depressed outer ring based on the depressed core-index.

Δn_1 (%)	Δn_2 (%)	Δn_3 (%)	Δn_4 (%)	Δn_5 (%)	r_1 (μm)	r_2 (μm)	r_3 (μm)	r_4 (μm)	r_5 (μm)
0.14	0.57	-0.27	0.30	-0.18	2.50	4.10	6.88	9.98	12.41

Table 6. Parameters of refractive index profile shown in Fig. 22

Table 7 shows the optical characteristic of fabricated fiber designed according to the refractive index profile parameters as Table 6, where MFD, RDS are the mode field diameter and relative

dispersion slope, respectively. It is noted that the fiber has a large A_{eff} of $105\text{ }\mu\text{m}^2$ and a small dispersion slope of about 0.065 ps/km/nm^2 simultaneously. Macro bending loss at 1550 nm is less than 0.05 dB/km (100 turns on the 60 mm diameter mandrel).

Parameters item	Wavelength (nm)	Typical value
Dispersion (ps/km/nm)	1460	3.465
	1550	9.569
	1625	14.324
Dispersion Slope(ps/km/nm ²)	1550	0.0648
Zero dispersion wavelength (nm)	-	1413
Attenuation (dB/km)	1550	0.210
MFD (μm)	1550	10.2
A_{eff} (μm^2)	1550	105.6
$A_{\text{eff}} \times \text{dispersion}$	1550	1010.5
RDS (nm ⁻¹)	1550	0.0068
PMD(ps/km ^{0.5})	1550	0.04
Macro bending loss for 100 turns on the 60mm diameter (dB/km)	1550	0.006
	1625	0.015

Table 7. Optical characteristics of the fabricated fiber

From the table7 we can see that the zero dispersion wavelength is below 1430 nm , the dispersion at $1460, 1550$ and 1625 nm are $3.465, 9.569$ and 12.324 ps/km/nm , respectively. Therefore, this fiber not only can be used at the conventional C band for transmission link, but also can be suited for S-band and L-band. With the progress being made in the practical application of the Raman amplifier, this fiber also can be applicable in transmission links using distributed Raman amplifier in the future. Furthermore, the value of $A_{\text{eff}} \times \text{dispersion}$ is also large enough to suppress the dispersion-related non-linear effects in the transmission system [35]. It is obvious that a large effective area fiber with non-zero dispersion about 4 ps/km/nm at $1.55\text{ }\mu\text{m}$ wavelength band is a good approach to avoid four-wave mixing (FWM) effect, which in turn enhances the performance of wavelength division multiplexing (WDM) system [31]. However, such large effective area fibers have relatively large dispersion slope which also restricts the numbers of different wavelength signals [21, 36-38]. Therefore, considerable efforts are being made to reduce the dispersion slope of such fibers to deal with a rapid progress of DWDM system [39,40]. The refractive index profile of the fiber is shown in Fig. 23. This profile has been named RI type in the literatures. In order to obtain the flat modal field over the entire central dip region, the effective index (n_{eff}) of the mode should be equal to the refractive index of the central dip (i.e., $n_{\text{eff}} = n_1$) [15]. The values of various parameters used in design of the dispersion characteristics are tabulated in Table 8. Here, the relative index difference Δi is given by $\Delta i = (n_i^2 - n_4^2) / 2n_i^2, i = 1, 2, 3$. The values of the MFD and A_{eff} associated with the modal field of the proposed design are $8.3\text{ }\mu\text{m}$ and $56.1\text{ }\mu\text{m}^2$, respectively. The total dispersion coefficient (D), which includes both waveguide and material dispersion of the fiber, is calculated in the wavelength range of 1530 to 1610 nm , which covers the entire C- and L-bands of erbium doped fiber amplifiers. In order to study the tolerance of the various characteristics of the proposed fiber design, we have randomly changed the values of thickness and Δ of each region by 1% . The actual and

the corresponding perturbed refractive index profiles are shown schematically in Fig. 23 by the solid and dashed curves, respectively. Figure 24 shows the variation of the total dispersion (D) with wavelength. The solid and dashed curves correspond to the actual and the perturbed refractive index profiles, respectively. This figure indicates that over the entire wavelength range of 1530 to 1610 nm, the dispersion value, which is within 2.6–3.4 ps/km/nm, for both profiles are within the appropriate range (2–4 ps/km/nm) needed to avoid four wave mixing (FWM) [41].

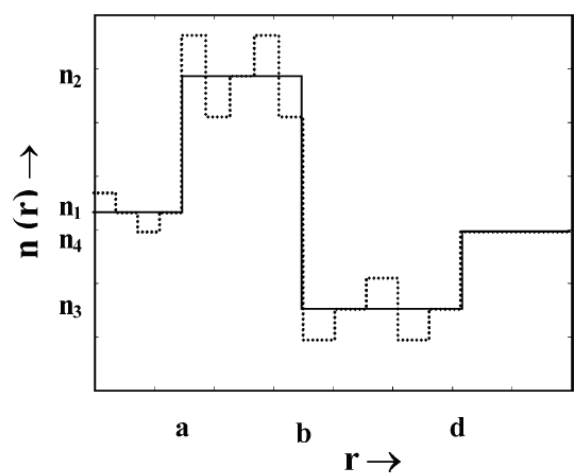


Fig. 23. Schematic of the refractive index profiles of the proposed fiber (solid curve). The dashed curve corresponds to the perturbed refractive index profile.

$a(\mu\text{m})$	$b(\mu\text{m})$	$d(\mu\text{m})$	$\Delta_1(\%)$	$\Delta_2(\%)$	$\Delta_3(\%)$
1.0	3.1	6.5	0.03	0.48	-0.20

Table 8. The values of various parameters used in design

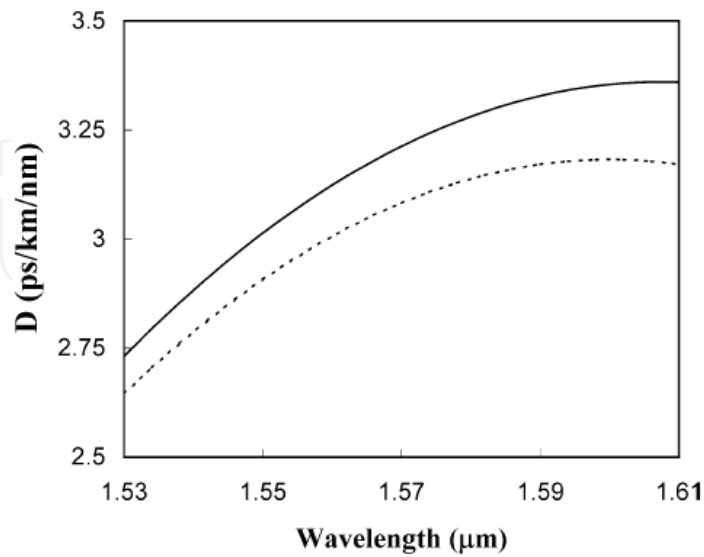


Fig. 24. Variation of the total dispersion (D) as a function wavelength. The solid and dashed curves correspond to the proposed and the perturbed refractive index profiles (shown schematically in Fig. 23), respectively.

The dispersion and dispersion values of the designed fiber at $\lambda_0 = 1550$ nm is 3.0 ps/km/nm and 0.01 ps/km/nm², respectively. The maximum value of dispersion slope is 0.015 and 0.014 ps/km/nm² for the actual and perturbed refractive index profiles over the entire wavelength range of 1530 to 1610 nm. This shows that the perturbation in the refractive index profile does not make much change in the dispersion slope.

9. Dispersion Flattened Fibers (DFFs)

The dispersion value becomes larger by the wavelength increasing in the conventional optical fibers. So owing to the dissimilar broadening for different channels, the multi-channel application realization would be hard. A suitable optical fiber should meet the small dispersion as well as the small dispersion slope in the predefined wavelength interval [42]. The concept of providing the attractive option of low dispersion over a range of wavelengths was first suggested by Kawakami and Nishida in 1974 [43, 44]. They proposed the original "W" fiber structure and explained the importance of a relatively narrow depressed cladding region in modifying the waveguide dispersion to give a curve which turned over to give two wavelengths for zero dispersion [45]. To minimize pulse broadening in an optical fiber, the chromatic dispersion should be low over the wavelength range used. A fiber in which the chromatic dispersion is low over a broad wavelength range is called a dispersion-flattened fiber. The rms value, or the function f , to be minimized is:

$$f = \left(\frac{1}{\lambda_2 - \lambda_1} \int_{\lambda_1}^{\lambda_2} C^2(\lambda_0) d\lambda_0 \right)^{1/2} \quad (13)$$

where C is the chromatic dispersion. A normalized W profile is given by

$$N(r) = \begin{cases} N_1 & 0 \leq r < b \\ N_2 & b \leq r < a \\ 1 & r \geq a \end{cases} \quad (14)$$

where $N_1 > 1$ and $N_2 < 1$. The constraint that the first higher-order mode should appear exactly at 1.25 μm is imposed. Thus there are four variables, namely, (N_1, N_2, b, a) , and one constraint. Assume that N_1 and N_2 are given certain fixed values. The values $N_1 = 1.02$ and $N_2 = 0.99$ will prove to be interesting. If $b = a$, then the W profile has degenerated into a step-index profile. The core radius, a , of this step-index fiber is easily calculated with the exact cutoff condition $V = 2.405$, where V is the normalized frequency. The value $N_1 = 1.02$ yields $b = a = 1.64 \mu\text{m}$. Direct numerical calculation shows that if the outer radius, a , is increased then the inner radius, b , must also be increased to keep the cutoff wavelength at 1.25 μm . Hence the constraint $\lambda_c = 1.25 \mu\text{m}$ corresponds to a curved line in the a - b plane. The rms value of the chromatic dispersion along this line is given in Fig. 25. The point of minimum dispersion is easily located.

This procedure is repeated for different combinations of N_1 and N_2 , and the result is given in Table 9. The first column of this table, i.e., $N_2 = 1$, corresponds to step-index profiles.

According to Table 9, the global minimum is 0.9 ps/km /nm, and the corresponding optimal W fiber is $(N_1, N_2, b, a) = (1.02, 0.99, 1.91, \text{ and } 2.85 \mu\text{m})$; see Fig. 26. It should be observed that the global minimum is flat; i.e., there is a valley in Table 9 giving roughly the same rms dispersion. Another observation is that the dependence of N_2 in Table 9 is weak if N_1 is less than 1.01. On the other hand, the dependence of N_2 is strong if N_1 is greater than 1.01 and N_2 is close to unity.

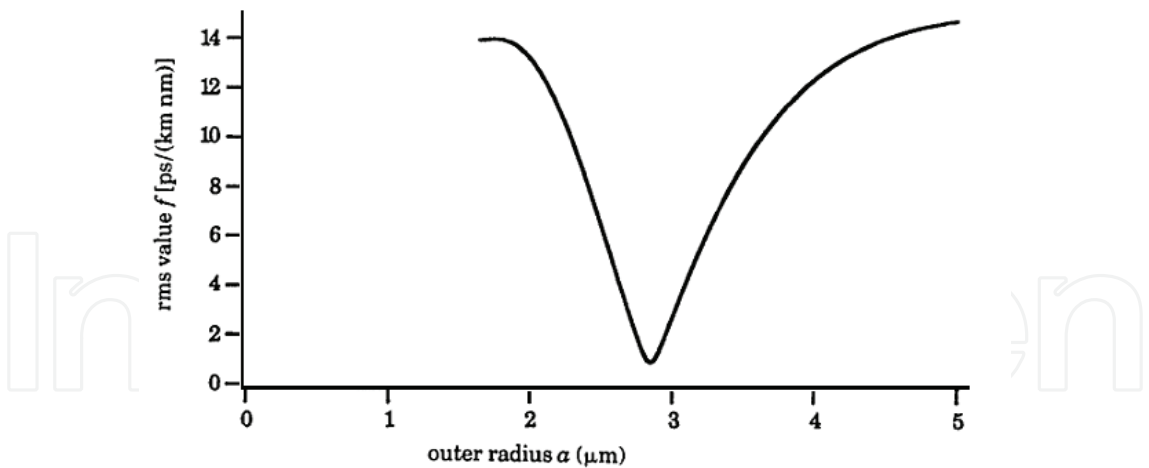


Fig. 25. The rms value of the chromatic dispersion over the vacuum wavelength range (1.25 μm , 1.60 μm) as a function of the outer radius a in a W fiber. The cutoff vacuum wavelength is 1.25 μm . The relative refractive-index increases in the core and in the inner cladding are 1.02 and 0.99, respectively.

	N ₂				
N ₁	1.000	0.995	0.990	0.985	0.980
1.002	12	12	12	12	12
1.005	8.6	8.6	8.5	8.5	8.5
1.010	4.8	4.3	4.2	4.1	4.1
1.015	7.9	2.3	1.8	1.6	1.5
1.020	14	1.3	0.9	1.0	1.2
1.025	21	1.1	1.7	2.4	2.9
1.030	27	4.0	2.4	3.7	4.5

Table 9. Minimum rms chromatic dispersion (ps/km/nm) for different doping level in the core & cladding

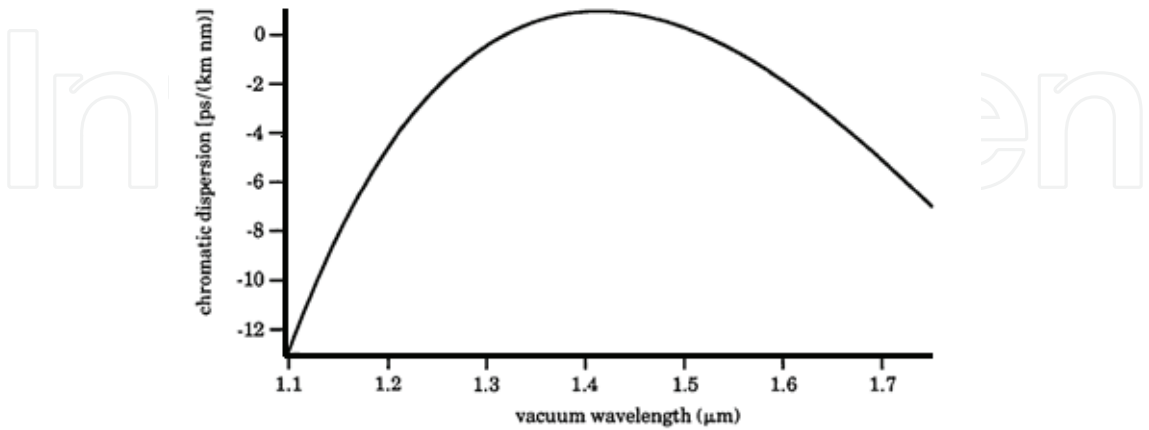


Fig. 26. Chromatic dispersion for the optimal W fiber (N_1, N_2, b, a) = (1.02, 0.99, 1.91 μm , 2.85 μm). The rms value of the chromatic dispersion over the vacuum wavelength range (1.25 μm , 1.60 μm) is equal to 0.9 ps/km/ nm. The cutoff vacuum wavelength is 1.25 μm .

An exhaustive method for calculating the minimum rms chromatic dispersion in W fibers has been presented [45]. The procedure is to generate all W fibers with a certain cutoff wavelength and then find the minimum rms dispersion by one-dimensional minimization followed by direct inspection. It was found, in the case investigated, that the W fiber is capable of dispersion flattening only if high doping levels are used. Dispersion and its slope are responsible on the pulse broadening [4]. So we believe that mixing and gathering these parameters on the design procedure would lead us to a fiber with exciting performances. In other words, we concentrate on dispersion and slope simultaneously to achieve the small dispersion and its slope in the predefined wavelength interval, the band which we want to have flat dispersion behavior [42]. We use WII-type optical fiber structure which its refractive index profile is shown in Fig. 27.

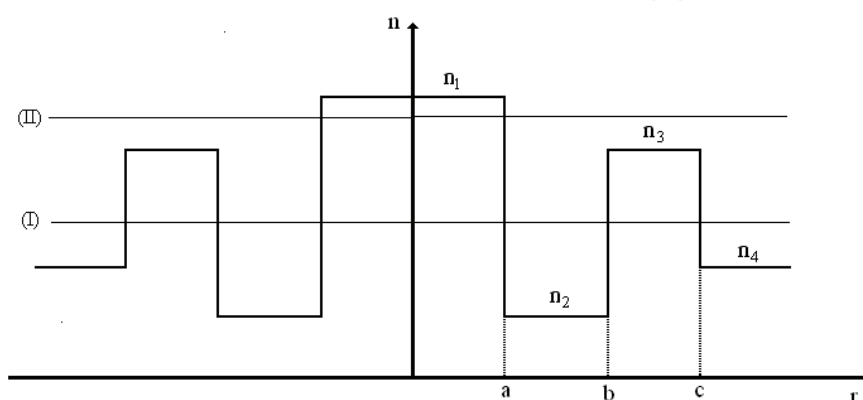


Fig. 27. The index of refraction profile for the proposed structures (WII)

Also, for easy handling of the problem the following optical parameters are defined as follows.

$$R_1 = \frac{n_1 - n_3}{n_3 - n_2}, R_2 = \frac{n_2 - n_4}{n_3 - n_2}, \Delta = \frac{n_1^2 - n_4^2}{2n_4^2} \approx \frac{n_1 - n_4}{n_4}. \quad (15)$$

For this structure the geometrical parameters are introduced in the following.

$$P = \frac{b}{c}, Q = \frac{a}{c}. \quad (16)$$

To achieve the flattening purpose, we have defined a weighted fitness function. Equation (17) shows our proposal for the weighted fitness function of the un-chirped pulse broadening factor.

$$F = \sum_{\lambda} e^{-\frac{(\lambda - \lambda_0)^2}{2\sigma^2}} \sum_Z [1 + (\frac{\beta_2(\lambda)Z}{t_i^2})^2 + (\frac{\beta_3(\lambda)Z}{2t_i^3})^2]^{\frac{1}{2}}, \quad (17)$$

It is useful to say that at first we applied this fitness function to design dispersion shifted fiber. But outcomes presentation will show that this function is appropriate in Flattening application too [42]. By using this fitness function, the zero dispersion wavelength can be shifted to the central wavelength (λ_0). Since, the weight of the pulse broadening factor at λ_0 is greater than others in the weighted fitness function; it is more likely to find the zero

dispersion wavelength at λ_0 compared to the other wavelengths. In the meantime, the flattening of the dispersion curve is controlled by Gaussian parameter (σ). To put it in another way, the weighting Gaussian function becomes broader in the predefined wavelength interval by increasing the Gaussian parameter (σ). As a result, the effect of the pulse broadening factor with greater value is regarded in different wavelengths, which causes a considerable decrease in the dispersion slope in the interval. Consequently, the zero dispersion wavelength and dispersion slope can be tuned by λ_0 and σ , respectively. The wavelength and the distance durations for the design are defined as follows: $1.50 \mu\text{m} < \lambda < 1.60 \mu\text{m}$; $0 < z < 200 \text{ km}$. In the simulations un-chirped initial pulse with 5 ps as full-width at half-maximum is used. From Figure 28, it is clear that the zero dispersion wavelength is successfully set at λ_0 which is equal to $1.55 \mu\text{m}$. Furthermore, the dispersion curve becomes so flat by adding the Gaussian weighting term to the fitness function. In other words, in the absence of weighting function, the optimized dispersion has higher slope compared to its presence.

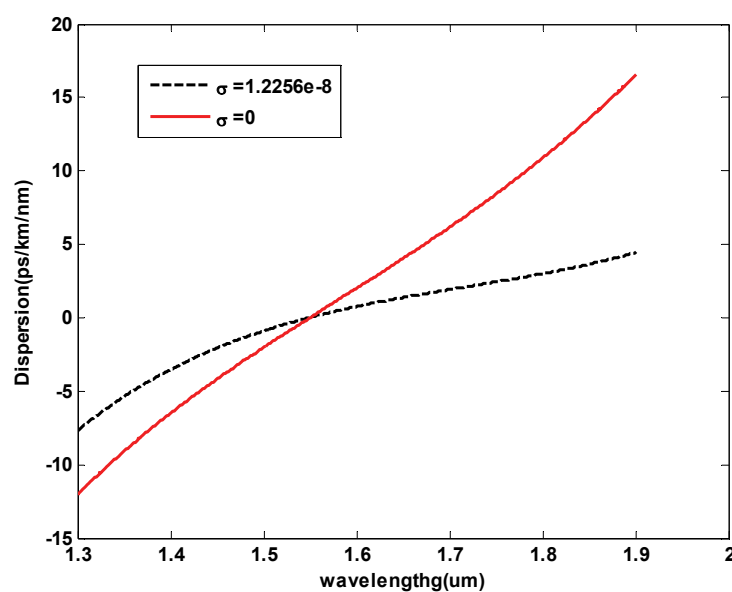


Fig. 28. Dispersion versus Wavelength with and without weighting function

The impact of sigma parameter on the dispersion and its slope is illustrated in Figures 29 and 30. It is obvious that the dispersion value reduces by the sigma parameter increase in the predefined wavelength interval and the curve is the smoothest in the highest sigma case. This event can be described based on the fact that the weighting function (Gaussian function) has large values around the central wavelength by the increase in the Gaussian parameter. So, a large band of the wavelength around the central wavelength has almost the same chance for optimization and thus the dispersion will be small and uniform for this band. In other words, the duration of this band can be controlled by the sigma parameter.

The dispersion slope is strongly affected by the presence of σ in such a manner that its increase has the considerable influence on the dispersion slope and decreases it obviously. This result is easily visible in Figure 30 which shows the dispersion slope versus wavelength with variance of the σ as a parameter. According to the presented weighted function based GA optimization, the following optical and geometrical parameters are obtained. We find out that the optimal value of R_2 for all Gaussian parameters are near to -1.

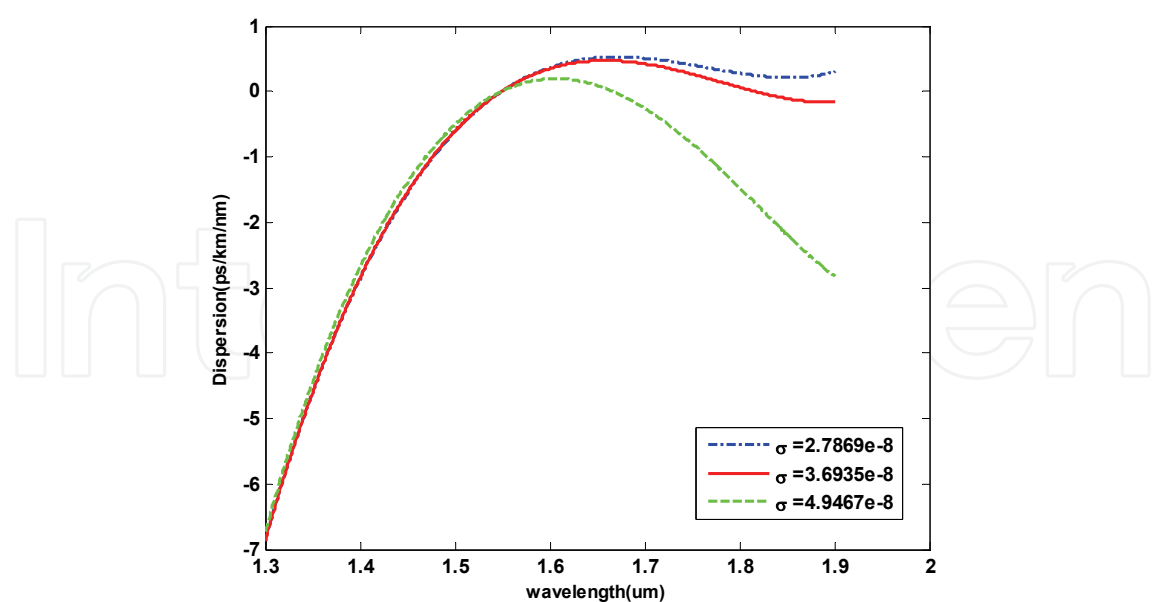


Fig. 29. Dispersion versus Wavelength for different Gaussian parameter

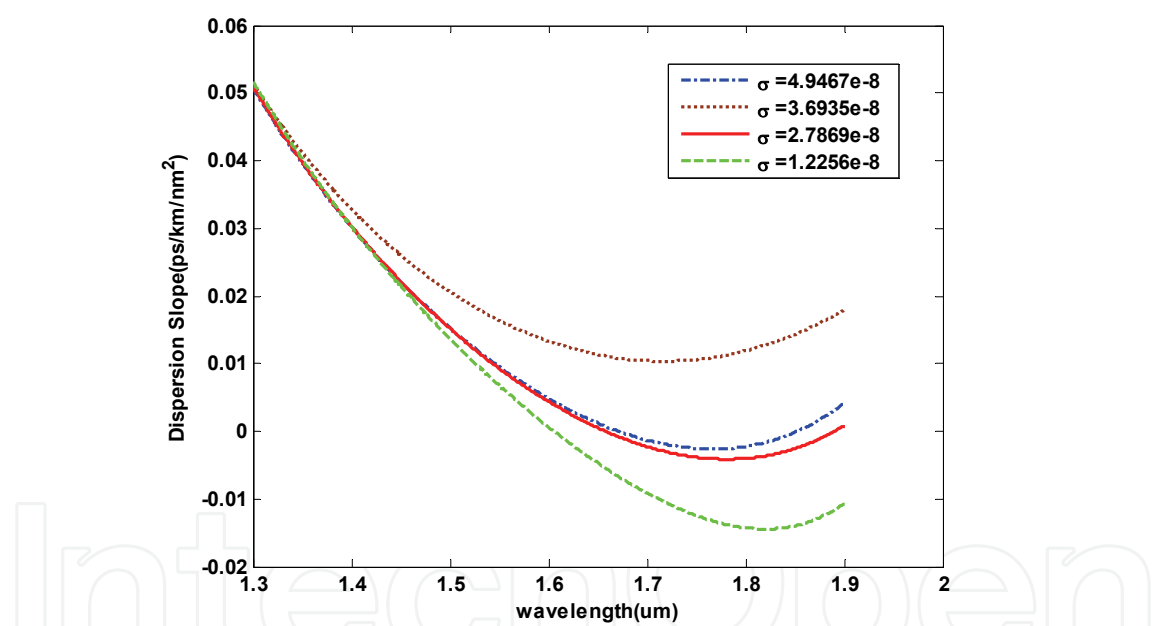


Fig. 30. Dispersion Slope versus Wavelength for different Gaussian parameter

<i>type</i>	<i>a</i> (<i>μm</i>)	<i>P</i>	<i>Q</i>	<i>R</i> ₁	<i>R</i> ₂	<i>Δ</i>
<i>σ</i> = 0 .00	2.5462	0.6942	0.3046	7.0897	-0.9517	4.886e-3
<i>σ</i> = 1.2256 <i>e</i> − 8	2.4450	0.7189	0.4049	3.0497	-0.9854	8.159e-3
<i>σ</i> = 2.7869 <i>e</i> − 8	2.5763	0.8478	0.4774	2.2437	-0.9877	7.178e-3
<i>σ</i> = 3.6935 <i>e</i> − 8	2.4374	0.8461	0.4098	1.7966	-0.7076	8.064e-3
<i>σ</i> = 4.9467 <i>e</i> − 8	2.5914	0.8942	0.4728	2.2583	-0.9780	6.812e-3

Table 10. Optimal Values for the Optical and Geometrical Parameters

In tables 11 and 12 the simulated numerical values of dispersion and dispersion slope based on the presented algorithm for wavelength duration in $[1.5-1.6]\mu m$ are given. Also, dispersion and dispersion slope difference for this band are presented for each case. For these cases, we show that there is about 6 times difference between traditional optimization and weighted function based optimization in dispersion case.

<i>type</i>	$D(\lambda = 1.5\mu m)$ <i>ps / km / nm</i>	$D(\lambda = 1.55\mu m)$ <i>ps / km / nm</i>	$D(\lambda = 1.6\mu m)$ <i>ps / km / nm</i>	$\Delta D = D(1.6) - D(1.5)$ <i>ps / km / nm</i>
$\sigma = 0.00$	-2.039	-0.032e-3	2.002	4.041
$\sigma = 1.2256e-8$	-0.899	0.0238	0.765	1.664
$\sigma = 2.7869e-8$	-0.618	0.0032	0.363	0.981
$\sigma = 3.6935e-8$	-0.606	0.0051	0.346	0.952
$\sigma = 4.9467e-8$	-0.510	0.0034	0.191	0.701

Table 11. Simulated Numerical Results for Dispersion for wavelength duration $[1.5-1.6]\mu m$

<i>type</i>	$S(\lambda = 1.5\mu m)$ <i>ps / km / nm²</i>	$S(\lambda = 1.55\mu m)$ <i>ps / km / nm²</i>	$S(\lambda = 1.6\mu m)$ <i>ps / km / nm²</i>
$\sigma = 0.00$	0.0416	0.0402	0.0401
$\sigma = 1.2256e-8$	0.0206	0.0164	0.0133
$\sigma = 2.7869e-8$	0.0153	0.0096	0.0488
$\sigma = 3.6935e-8$	0.0152	0.0093	0.0044
$\sigma = 4.9467e-8$	0.0137	0.0068	0.0007

Table 12. Simulated Numerical Results for Dispersion Slope for wavelength duration $[1.5-1.6]\mu m$

As a final result of these simulations, we should point out that for zero value of the Gaussian parameter zero-dispersion wavelength has high accuracy compared to nonzero-values of the Gaussian parameters cases. By comparing presented results and the ones demonstrated earlier as a dispersion flattened optical fiber, it is clear that the least design has considerable band width, the band between to zero dispersion wavelength. Moreover, the dispersion value tolerance in this interval is so small which is a direct result of its small slope.

10. Conclusion

In this chapter some special fiber structures for covering broadband optical fiber communications were reviewed. For these three cases R, W and M two different types for each of them were considered and discussed in detail. We have been shown that using the proposed design method in this chapter systematic approach for broadband applications can be found and considering the fibers in this chapter ultra broadband communications are available.

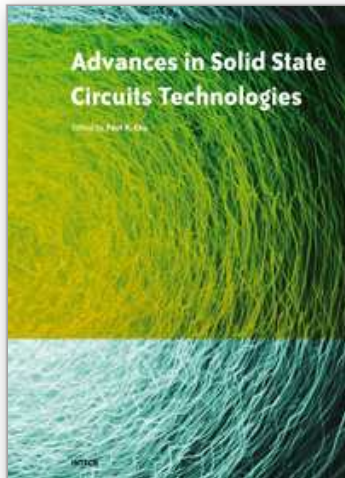
11. References

- [1] kazumasa Ohsono, Tomoyuki Nishio, Takahiro Yamazaki, Tomomi Onose, and Kotaro Tan, "Low Non-linear Dispersion-shifted Fiber for DWDM Transmission", HITACHI CABLE REVIEW, Vol. 19, 2000.
- [2] J. A. Baghdadi, A. Safaai-Jazi, and H.T. Hattori, "Optical fibers with low nonlinearity and low polarization-mode dispersion for terabit communications," Optics & Laser Technology, Vol. 33, pp. 285-291, 2001.
- [3] S. Makouei, M. savadi-Oskouei, A. Rostami, and Z.D.K. Kanani, "DISPERSION FLATTENED OPTICAL FIBER DESIGN FOR LARGE BANDWIDTH AND HIGH-SPEED OPTICAL COMMUNICATIONS USING OPTIMIZATION TECHNIQUE", Progress In Electromagnetics Research B, Vol. 13, pp. 21-40, 2009.
- [4] Govind P. Agrawal, "Fiber-Optic Communication Systems", (John Wiley & Sons, Third Edition), 2002.
- [5] T. Kato, M. Hirano, A. Tada, K. Fukuada, T. Fujii, T. Ooishi, Y. Yokoyama, M. Yoshida, and M. Onishi, "Dispersion flattened transmission line consisting of wide-band non-zero dispersion shifted fiber and dispersion compensating fiber module", Optical Fiber Technology, Vol. 8, pp. 231-239, 2002.
- [6] R. Tewari, B.P. Pal, and U.K. Das, "Dispersion shifted dual shape core fibers: Optimization based on spot size definitions" , Lightwave Technology, vol. 10, pp. 1-5, 1992.
- [7] Dipankar Ghosh, Debashri Ghosh, and Mousumi Basu, "Designing a graded index depressed clad non-zero dispersion shifted optical fiber for wide band transmission system", Optik Optics, vol. 119, pp. 63-68, 2008.
- [8] B. Mikkelsen, G. Raybon, B. Zhu, R.J. Essiambre, P.G. Bernasconi, K. Dreyer, L.W. Stulz, S.N. Knudsen, " High spectral efficiency (0.53 bit/s/Hz) WDM transmission of 160 Gb/s per wavelength over 400 km of Fiber", Technical Digest of OFC 2001, 2001, Paper ThF2.
- [9] T. Ito, K. Fukuchi, K. Sekiya, D. Ogasawara, R. Ohhira, T. Ono, " 6.4 Tb/s (160 × 40 Gb/s) WDM transmission experiment with 0.8 bit/s/Hz spectral efficiency" , ECOC 2000, 2000, Postdeadline paper PD1.1.
- [10] J. Kani, K. Hattori, M. Jinno, T. Kanamori, K. Oguchi, " Tripple-wavelength-band WDM transmission over cascaded dispersion-shifted fibers", Technical Digest of OAA'99, 1999, Paper WC2.
- [11] K. Fukuchi, T. Kasamatsu, M. Morie, R. Ohhira, T. Ito, K. Sekiya, D. Ogasawara, T. Ono, "10.92-Tb/s (273 × 40-Gb/s) triple-band/ultra-dense WDM optical-repeated transmission experiment", OFC 2001, Postdeadline paper PD24, 2001.
- [12] A. Naka et al., Lightwave Technol., vol.12, no.2, February (1994) pp. 280-287
- [13] Y. Liu et al., OFC'96, WK15, 1996.
- [15] R.K. Varshney, A.K. Ghatak, I.C. Goyal, and C. siny Antony, "Design of a flat field fiber with very small dispersion slope," Optical Fiber Technology, vol. 9, pp. 189-198, 2003.
- [16] J. Sakamoto, J. Kani, M. Jinno, S. Aisawa, M. Fukui, M. Yamada, K. Oguchi, "Wide wavelength band (1535–1560 nm and 1574–1600 nm), 28 × 10 Gbit/s WDM transmission over 320 km dispersion shifted fiber", Electron. Letter, vol. 34, pp. 392-394, 1998.

- [17] S. Yashida, S. Kuwano, K. Iwashita, "10 Gbit/s \times 10 channel WDM transmission experiment over 1200 km with repeater spacing of 100 km without gain equalization or pre-emphasis", Optical Fiber Communication (OFC') 96, San Jose, CA, TuD6, 1996.
- [18] A.R. Chraplyvy, "Limitation on lightwave communications imposed by optical fiber nonlinearities", Lightwave Technology, vol. 8, pp. 1548-1557, 1990.
- [19] R.W. Tkach, A.R. Chraplyvy, F. Fabrizio, A.H. Gnauck, R.M. Derosier, "Four photon mixing and high speed WDM systems", Lightwave Technology, vol. 13, pp. 841-849, 1995.
- [20] Y. Akasaka, "New optical fibers for high bit rate and high capacity transmission", SPIE Proc., Vol. 3666, pp. 23-29, 1999.
- [21] Y. Liu, A.J. Antos, V.A. Bhagavatula, M.A. Newhouse, "Single mode dispersion shifted fiber with effective area larger than 80 μm^2 and good bending performance", Proc. of ECOC'95, TuL2.4, 1995.
- [22] M. Tateda, Y. Kato, S. Seikai, and N. Uchida, "Design consideration on single mode fiber parameters," Pans. IECE Japan, (in Japanese) vol. J56-B, pp. 324-331, 1982.
- [23] K.I. Kitayama, Y. Kato, M. Ohashi, Y. Ishida, and N. Uchida, "Design considerations for the structural optimization of a single mode fiber," Lightwave Technology, vol. 1, pp. 363-369, 1983.
- [24] M. Savadi-Oskouei, S. Makouei, A. Rostami, and Z.D. Koozeh Kanani, "Proposal for optical fiber designs with ultrahigh effective area and small bending loss applicable to long haul communications", applied Optics, vol. 46, pp. 6330-6339, 2007.
- [25] Y. Namihiro, "Relationship between nonlinear effective area and mode-diameter for dispersion shifted fiber," Electron. Letter, vol. 30, pp. 262-264, 1994.
- [26] M. Hautakorpi and M. Kaivola, "Modal analysis of M-type dielectric-profile optical fibers in the weakly guiding approximation," Optical Society of America A., vol. 22, pp. 1163-1169, 2005.
- [27] F. D. Nunes and C. A. de Souza Melo, "Theoretical study of coaxial fibers," Applied Optics, vol. 35, pp. 388-398, 1996.
- [28] D. E. Goldberg, *Genetic Algorithms in Search, Optimization and Machine Learning* (Addison-Wesley, 1989).
- [29] X. Tian and X. Zhang, "Dispersion flattened design of large effective area single mode fibers with ring index profiles", Optics Communications, vol. 230, pp. 105-113, 2004.
- [30] Z. O. Tseng, "On the Convergence of the Coordinate Descent Method for Convex Differentiable Minimization", Optimization Theory and Applications, vol. 72, pp. 7-35, 1992.
- [31] S. Yin, K.w. Chung, H. Liu, P. Kurtz, and K. Reichard, "A new design for non-zero dispersion shifted fiber (NZ-DSF) with a large effective area over 100 μm^2 and low bending and splice loss", Optics Communications, vol. 177, pp. 225-232, 2000.
- [32] X. Jiang and R. Wang, "Non-zero dispersion shifted optical fiber with ultra large effective area and low dispersion slope for terabit communication systems", optics Communications, vol. 236, pp. 69-74, 2004.
- [33] B.H. Kim, Y. Park, D.Y. Kim, U.C. Paek, W.-T. Han, in: OFC_2002, Technical Digest, 2002, pp. 173-174.
- [34] U.C. Pack, C.R. Kurkjian, J. Am. Ceram. Soc. 58 (1975)330.

- [35] S. Matsuo, S. Tanigawa, K. Himeno, K. Harada, in: OFC_2002, Technical Digest, 2002, pp. 329–330.
- [36] A. Safaai-Jazi, "Large effective area fibers: propagation properties and optimum designs", SPIE Proc., Vol. 3666, pp. 30–39, 1999.
- [37] P. Nouchi, P. Sansonetti, J. Von Wirth, and C. Le Sergeant, "New dispersion shifted fiber with effective area larger than $90 \mu\text{m}^2$ ", Proc. of ECOC'96, MoB3.2, 1996.
- [38] V. Silva, "A new design for dispersion shifted fiber with an effective area larger than $100 \mu\text{m}^2$ and good bending characteristics", Proc. of OFC'98, ThK1, p. 301, 1998.
- [39] N. Kumano, K. Mukasa, S. Matsushita, T. Yagi, "Zero dispersion slope NZ-DSF with ultra wide bandwidth over 300 nm", Proc. of ECOC'2002, 2002.
- [40] B. Zhu, L.E. Nelson, L. Leng, S. Stulz, S. Knudsen, D. Peckham, "1.6 Tbits/s (40×42.7 Gbit/s) WDM transmission over 2400 Km of fiber with 100 Km dispersion managed spans", Electron. Letters, vol. 38, pp. 647–648, 2002.
- [41] P. Nouchi, P. Sansonetti, J. Von Wirth, C. Le Sergeant, "New dispersion shifted fiber with effective area larger than $90 \mu\text{m}^2$ ", Proc. of ECOC'96, MoB3.2, 1996.
- [42] M. Savadi-Oskouei, A. Rostami, and S. Makouei, "A novel fiber design strategy for simultaneously introducing ultra small dispersion and dispersion slope using genetic algorithm", European Transaction on Telecommunications, vol. 20, pp. 37–47, 2009.
- [43] S. Kawakami and S. Nishida, "Anomalous dispersion of new doubly clad optical fibers", Electron Letters, vol. 10, pp. 38–40, 1974.
- [44] S. Kawakami, S. Nishida, and M. Sumi, "Transmission characteristics of W-type optical fibers", Proc. Inst. Elec. Eng., vol. 123, pp. 586–590, 1976.
- [45] B. James and C.R. Day, "A review of single mode fibers with modified dispersion characteristics", Lightwave Technology, vol. 4, pp. 967–979, 1986.

IntechOpen



Advances in Solid State Circuit Technologies

Edited by Paul K Chu

ISBN 978-953-307-086-5

Hard cover, 446 pages

Publisher InTech

Published online 01, April, 2010

Published in print edition April, 2010

This book brings together contributions from experts in the fields to describe the current status of important topics in solid-state circuit technologies. It consists of 20 chapters which are grouped under the following categories: general information, circuits and devices, materials, and characterization techniques. These chapters have been written by renowned experts in the respective fields making this book valuable to the integrated circuits and materials science communities. It is intended for a diverse readership including electrical engineers and material scientists in the industry and academic institutions. Readers will be able to familiarize themselves with the latest technologies in the various fields.

How to reference

In order to correctly reference this scholarly work, feel free to copy and paste the following:

Rostami and S. Makouei (2010). A Novel Multiclad Single Mode Optical Fibers for Broadband Optical Networks, *Advances in Solid State Circuit Technologies*, Paul K Chu (Ed.), ISBN: 978-953-307-086-5, InTech, Available from: <http://www.intechopen.com/books/advances-in-solid-state-circuit-technologies/a-novel-multiclad-single-mode-optical-fibers-for-broadband-optical-networks>

INTECH
open science | open minds

InTech Europe

University Campus STeP Ri
Slavka Krautzeka 83/A
51000 Rijeka, Croatia
Phone: +385 (51) 770 447
Fax: +385 (51) 686 166
www.intechopen.com

InTech China

Unit 405, Office Block, Hotel Equatorial Shanghai
No.65, Yan An Road (West), Shanghai, 200040, China
中国上海市延安西路65号上海国际贵都大饭店办公楼405单元
Phone: +86-21-62489820
Fax: +86-21-62489821

© 2010 The Author(s). Licensee IntechOpen. This chapter is distributed under the terms of the [Creative Commons Attribution-NonCommercial-ShareAlike-3.0 License](https://creativecommons.org/licenses/by-nc-sa/3.0/), which permits use, distribution and reproduction for non-commercial purposes, provided the original is properly cited and derivative works building on this content are distributed under the same license.

IntechOpen

IntechOpen